Structural Analysis of Subdivision Surfaces – A Summary

Ulrich Reif and Jörg Peters

July 6, 2005

Abstract

This paper summarizes the structure and analysis of subdivision surfaces and characterizes the inherent similarities and differences to parametric spline surfaces. Besides presenting well known results in a unified way, we introduce new ideas for analyzing schemes with a linearly dependent generating system, and a significantly simplified test for the injectivity of the characteristic map.

1   Introduction

For a graphics designer, subdivision is a recipe for generating a finer and finer sequence of polyhedra that converges to a visually smooth limit surface after a few iteration steps (Figure 1). While this intuitive view accounts to a large extent for the success of subdivision in applications, it fails to provide a framework explaining the unique analytical structure of subdivision surfaces vis-a-vis other representations. In particular, this view, which was predominant in the early subdivision literature, fails to characterize the inherent similarities and differences to standard parametric spline surfaces.
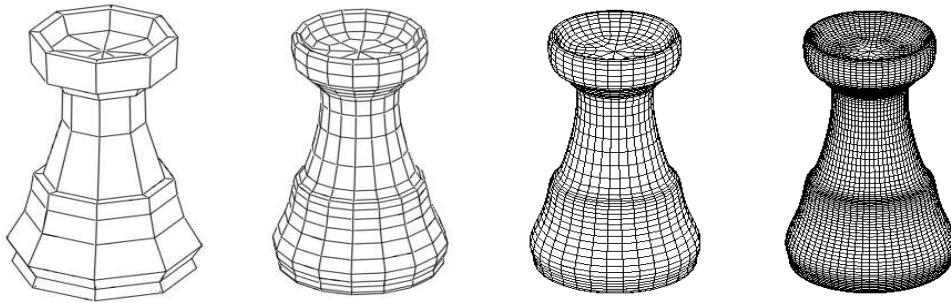

Figure 1: Four steps of Catmull-Clark subdivision (from [88]).

1

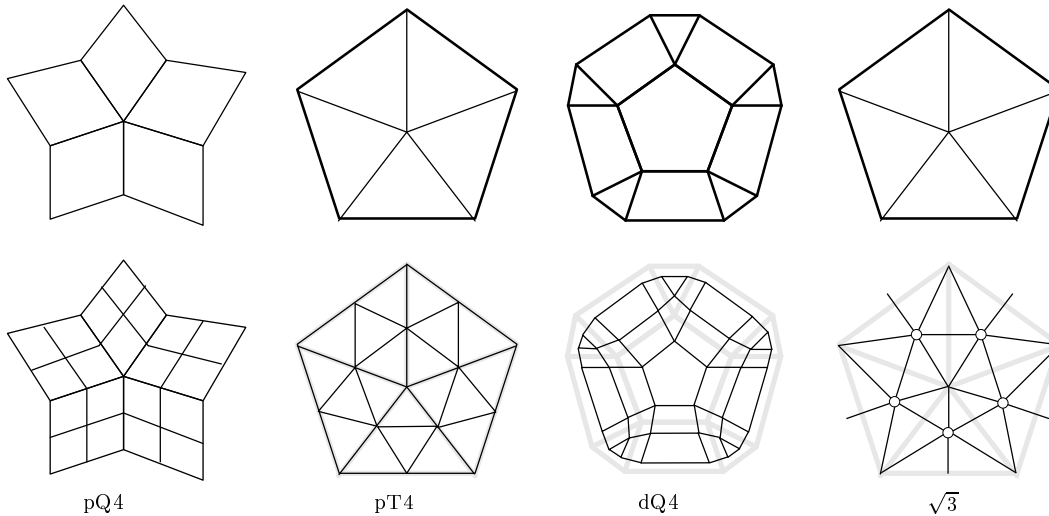pQ4   pT4   dQ4 $\sqrt{3}$

Figure 2: Refinement schemes (initial meshes *top*, refined meshes *bottom*). We focus on schemes of type pQ4 and dQ4 that result in quadrilateral patches; the analysis and structure of other subdivision schemes is analoguous.

To highlight the similarities, we use the term 'spline' in a much generalized sense. In the following, a spline is any function consisting of a finite or even infinite number of pieces, each of which is defined on an indexed copy of a standard domain. This definition covers in particular linear combinations of B-splines or box-splines. We focus on piecewise continuous functions defined on a union of *unit squares*; the analysis of spline surfaces over other, say triangular standard domains (see Figure 2), is analogous and need not be developed separately. To characterize continuity of a spline, its domain is endowed with the topological structure of a two-dimensional manifold. This avoids a more involved characterization by means of matching smoothness conditions for abutting patches.

To highlight the differences between spline surfaces and subdivision surfaces, we focus on the neighborhood of extraordinary points, e.g. points where $n \neq 4$ quadrilateral domains join. Here, the surface has the structure of a union of *spline rings*, i.e. circular annuli formed by matching up the boundaries of the spline patches (see Figure 5,*right*). (The word 'ring' will not lead to confusion since no rings in the algebraic sense will be considered in this paper.) The infinite sequence of nested surface rings no longer shares all properties of the underlying splines. For example, since these rings contract *ad infinitum*, it is necessary to use, in the limit, a differential geometric characterization of smoothness: smoothness is measured in a natural local coordinate system. Injectivity with respect to this coordinate system is crucial but not always present in subdivision schemes; and the lack of second-order differentiability with respect to the coordinate system presents a challenge for characterizing shape.

Contents. After defining splines, subdivision surfaces and algorithms, the paper characterizes increasing levels of continuity and correspondingly increasing restrictions on admissible schemes. The table of contents is as follows.

Sources. This article is the summary of a book on the structural analysis of subdivision surfaces [78], which is currently in preparation. At the end of each section, we give some bibliographical notes pointing to the most relevant and first-time references, without claiming completeness. In addition to the citations given in the article, we also include some further suggested reading on the topic in the list of references.

Notation. We use greek letters for objects in $\mathbb{R}^2$ and maps into $\mathbb{R}^2$ such as planar curves and reparametrizations. Bold face is used, in particular, for points and functions in the embedding space $\mathbb{R}^d$, $d > 2$. These points are understood as *row vectors* so that, following established practice in the literature, we apply $n \times n$ subdivision matrices from the left to a vector of n control points in $\mathbb{R}^d$. As in Matlab, elements in a row of a matrix or vector are separated by a comma, while rows are separated by a semicolon. For example,

$$[1,\ 2,\ 3;\ 4,\ 5,\ 6] = \begin{bmatrix} 1 & 2 & 3 \\ 4 & 5 & 6 \end{bmatrix}.$$
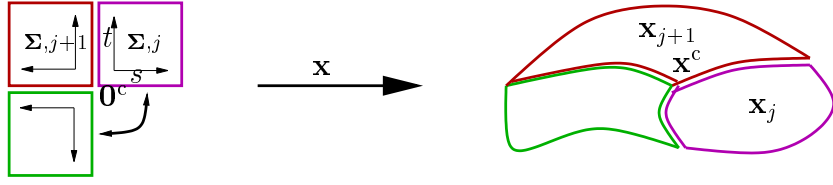
Figure 3: (*left*) Domain manifold $\boldsymbol{\Sigma} \times \mathbb{Z}_3$ and (*right*) spline manifold $\mathbf{x}$.

2 Spline surfaces near extraordinary points

To investigate surfaces with n quadrilateral pieces joining at a point, we define the unit interval in $\mathbb{R}$ and the unit square in $\mathbb{R}^2$, respectively:

$$U := [0,1] \quad \text{and} \quad \boldsymbol{\Sigma} := U \times U.$$

Then the domain $\mathbf{S}$,

$$\mathbf{S} := \boldsymbol{\Sigma} \times \mathbb{Z}_n, \quad \mathbb{Z}_n := \mathbb{Z} \mod n,$$

of a *spline* $\mathbf{x} : \mathbf{S} \to \mathbb{R}^d$ consists of n indexed copies of $\boldsymbol{\Sigma}$. Points in $\boldsymbol{\Sigma}$ and $\mathbf{S}$ are typically denoted

$$\boldsymbol{\sigma} = (s,t) \in \boldsymbol{\Sigma}, \quad \mathbf{s} = (\boldsymbol{\sigma}, j) = (s,t,j) \in \mathbf{S}.$$

The restriction of $\mathbf{x}$ to a single unit square with index j is called a *patch* and denoted $\mathbf{x}_j$:

$$\mathbf{x} : \mathbf{S} \ni (\boldsymbol{\sigma}, j) \mapsto \mathbf{x}_j(\boldsymbol{\sigma}) \in \mathbb{R}^d.$$

Now, pairs of edges of the unit squares are set equal according to

$$(0, u, j) = (u, 0, j+1), \quad u \in U, \ j \in \mathbb{Z}_n.$$

The common origin of all patch domains is

$$\mathbf{0}^{\mathrm{c}} := (\mathbf{0}, 0) = \cdots = (\mathbf{0}, n-1),$$

see Figure 3. The superscript "c" for "center" is used to tell the origin $\mathbf{0}^{\mathrm{c}}$ of $\mathbf{S}$ apart from the origin $\mathbf{0}$ of $\boldsymbol{\Sigma}$. By identifying edges of adjacent unit squares, the domain $\mathbf{S}$ becomes a simply connected topological space. Thus, there is a well-defined notion of continuity for splines. Due to the identification $(0, u, j) = (u, 0, j+1)$, the patches have to satisfy the *consistency conditions*

$$\mathbf{x}_j(0, u) = \mathbf{x}_{j+1}(u, 0), \quad j \in \mathbb{Z}_n,$$

and, in particular,

$$\mathbf{x}^{\mathrm{c}} := \mathbf{x}(\mathbf{0}^{\mathrm{c}}) = \mathbf{x}_0(\mathbf{0}) = \cdots = \mathbf{x}_{n-1}(\mathbf{0})$$

is called the *center* of $\mathbf{x}$. Subsequently, patches are always assumed to be continuous. Together with the consistency conditions, this implies that the spline $\mathbf{x} : \mathbf{S} \to \mathbb{R}^d$
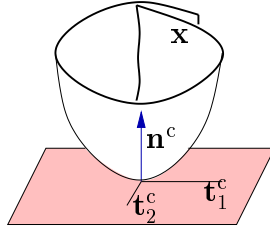
Figure 4: A normal continuous surface that is not single-sheeted.

is a continuous map. We will be interested in several choices of the dimension d of the image space. For $d = 3$, $\mathbf{x}$ is a *spline surface*, and this is the case we are eventually interested in. For $d = 2$, we obtain planar splines which are used for analytical purposes. Especially, the characteristic map to be defined later is of that type. Finally, for $d = 1$, we obtain real valued splines. We will use such splines to define generating systems for finite dimensional spline spaces in $\mathbb{R}^3$, just as B-splines are used to model standard tensor product spline surfaces. Next, we consider smoothness.

Definition 2.1 *A continuous spline* $\mathbf{x} : \mathbf{S} \to \mathbb{R}^d$ *is called* C_0^k, *if all patches* $\mathbf{x}_j$ *are* C^k-*functions on* $\mathbf{\Sigma} \backslash \{\mathbf{0}\}$, *and if the corresponding cross boundary derivatives at common edges are equal up to sign, i.e.,*

$$\partial_s^\nu \mathbf{x}_j(0, u) = (-1)^\nu \partial_t^\nu \mathbf{x}_{j+1}(u, 0), \quad \nu = 0, \ldots, k, \quad u \in (0, 1]. \tag{1}$$

The space of all C^k-*splines in* $\mathbb{R}^d$ *is denoted* $C_0^k(\mathbf{S}, \mathbb{R}^d)$.

Crucially, the central point is excluded from all smoothness conditions since, for $u = 0$, consistency implies, for $n \neq 4$ that either the partial derivatives of all patches vanish at the origin, or that the projection of $\mathbf{x}$ to the tangent plane at the origin is not injective. In the first case of a singular parametrization, the geometrical smoothness of the spline does not follow from the analytical smoothness of the parametrization; in the second case $\mathbf{x}$ cannot be a smooth surface in the sense of manifolds. As a consequence, we do not impose smoothness conditions at the center a priori. In essence, the rest of the paper deals with the challenge of reconciling the lack of smoothness in the parametrization of $\mathbf{x}$ with the geometric smoothness of its image. As a first step, we define normal continuity in the following way:

Definition 2.2 *A spline surface* $\mathbf{x} \in C_0^1(\mathbf{S}, \mathbb{R}^3)$ *is called* normal continuous *at the center, if the limit*

$$\mathbf{n}^c := \lim_{\mathbf{s} \to \mathbf{0}^c} \mathbf{n}(\mathbf{s})$$

of the Gauss map

$$\mathbf{n}(\mathbf{s}) := \tilde{\mathbf{n}}(\mathbf{s}) / \|\tilde{\mathbf{n}}(\mathbf{s})\|, \quad \tilde{\mathbf{n}}(\mathbf{s}) = \tilde{\mathbf{n}}(\boldsymbol{\sigma}, j) := \partial_s \mathbf{x}_j \times \partial_t \mathbf{x}_j$$

exists and is unique. In this case, $\mathbf{n}^c$ *is called the* central normal, *and the plane through* $\mathbf{x}^c$ *perpendicular to* $\mathbf{n}^c$ *is called the* central tangent plane.

5

It is easily shown that for a normal continuous spline surface $\mathbf{x} \in C_0^k(\mathbf{S}, \mathbb{R}^3)$, the Gauss map extended by $\mathbf{n}(\mathbf{0}^c) := \mathbf{n}^c$ is a spline in $C_0^{k-1}(\mathbf{S}, S^2)$, where S^2 is the unit sphere in $\mathbb{R}^3$. Normal continuity is not sufficient for a spline surface to be smooth in the sense of manifolds since the projection of $\mathbf{x}$ into the central tangent plane may not be injective. To address this problem, we choose two orthonormal vectors $\mathbf{t}_1^c, \mathbf{t}_2^c$ in the central tangent plane and collect them in a (2×3)-matrix $\mathbf{T}^c$. Then we define the *projection* $\boldsymbol{\xi}$ of $\mathbf{x}$ to that plane by

$$\boldsymbol{\xi} : \mathbf{S} \ni \mathbf{s} \mapsto (\mathbf{x}(\mathbf{s}) - \mathbf{x}^c) \cdot \mathbf{T}^c \in \mathbb{R}^2. \tag{2}$$

Here and subsequently, a dot denotes multiplication by the transpose,

$$\mathbf{A} \cdot \mathbf{B} := \mathbf{A}\mathbf{B}^{\mathrm{T}}.$$

$\mathbf{x}$ is called *single-sheeted* if $\boldsymbol{\xi}$ is injective when restricted to a sufficiently small neighborhood $\mathbf{S}'$ of the origin. In this case, we can use the inverse function $\mathbf{s} = \mathbf{s}(\boldsymbol{\xi})$ to define the *central height function* h on the set $\Xi' := \boldsymbol{\xi}(\mathbf{S}') \subset \mathbb{R}^2$ by

$$h : \Xi' \ni \boldsymbol{\xi} \mapsto (\mathbf{x}(\mathbf{s}(\boldsymbol{\xi})) - \mathbf{x}^c) \cdot \mathbf{n}^c \in \mathbb{R}. \tag{3}$$

With these settings, points on the spline surface near the center can be written as

$$\mathbf{x}(\mathbf{s}) = \mathbf{x}^c + \boldsymbol{\xi}\mathbf{T}^c + h(\boldsymbol{\xi})\mathbf{n}^c, \quad \mathbf{s} \in \mathbf{S}', \ \boldsymbol{\xi} \in \Xi',$$

and the geometrical smoothness of $\mathbf{x}$ at the center is just the analytical smoothness of h at the origin. If $\mathbf{x} \in C_0^1(\mathbf{S}, \mathbb{R}^3)$, then h is continuous on Ξ' and continuously differentiable on $\Xi' \backslash \{\mathbf{0}\}$. If, moreover, $\mathbf{x}$ is normal continuous, then one can show using the mean value theorem that h is also differentiable at the origin. Both value and gradient vanish there,

$$h(\mathbf{0}) = 0, \quad Dh(\mathbf{0}) = \mathbf{0}. \tag{4}$$

Definition 2.3 *A spline surface $\mathbf{x} \in C_0^k(\mathbf{S}, \mathbb{R}^3)$ is called C_r^k if it is single-sheeted, and if the central height function is r-times differentiable at the origin. The space of all C_r^k-splines is denoted $C_r^k(\mathbf{S}, \mathbb{R}^3)$.*

One should keep in mind that the superscript k refers to the smoothness of the parametrization, while the subscript r refers to the smoothness of the central height function at the origin. Strictly speaking, $\mathbf{x}$ can be a smooth manifold even if it is neither normal continuous in the sense of Definition 2.2 nor single-sheeted in the sense of Definition 2.3. As an example, consider the 'flat' spline $\mathbf{x}$ with patches

$$\mathbf{x}_0(\boldsymbol{\xi}) = \cdots = \mathbf{x}_{n-1}(\boldsymbol{\xi}) = r \sin(1/r) [\cos 4\varphi, \ \sin 4\varphi, \ 0],$$

where $\boldsymbol{\xi} = r(\cos \varphi, \ \sin \varphi)$. The normal vector, computed as the normalized cross product of partial derivatives, alternates between $[0, 0, 1]$ and $[0, 0, -1]$; and the projection of $\mathbf{x}$ to the xy-plane is not injective. Nevertheless, the image of $\mathbf{x}$ is simply a part of the xy-plane, hence a smooth manifold. We accept that such highly degenerate cases are not contained in the spaces $C_r^k(\mathbf{S}, \mathbb{R}^3)$.

Bibliographic Notes.

- The focus on spline surfaces consisting of quadrilateral patches is motivated by the Catmull-Clark-algorithm [9], the Doo-Sabin-algorithm [24], or the tensor-product four-point scheme [42, 47]. A completely analogous theory can be developed for triangular patches, as obtained for instance by Loop's scheme [52], the butterfly scheme [31], or $\sqrt{3}$-subdivision [45].

- Viewing the domain **S** as a topological space appears natural. Nevertheless, it was not explicitly introduced prior to [77, 98].

- An example for a surface which is normal continuous, but not single-sheeted can be found in [73].

- The conditions (1) are not necessary for a smooth join of the patches. Rather, it suffices to require coincidence of geometric quantities such as normal vectors, principal curvatures and directions, etc., at common edges. For a survey on the concept of so-called *geometric continuity* see, for instance, [58].

- The example of a degenerate parametrization of smooth manifolds elaborates on a remark in [99].

3   Subdivision surfaces defined

So far we have derived a general framework for splines near extraordinary points. Now we specialize it to the subdivision setting. In practice, subdivision surfaces are obtained by iterated refinement of control meshes. This refinement process enlarges the regular parts of the mesh, and scales down the central n-sided region near the extraordinary vertex. Since the limit surface corresponding to the regular parts of a mesh can at least in principle be determined explicitly, iterative refinement corresponds to the generation of a sequence of larger and larger parts of the final limit surface. Equally, one can represent the limit surface **x** as the union of the initially known regular part $\mathbf{x}^0$ and a sequence of ring-shaped parts $\mathbf{x}^m, m \in \mathbb{N}$, which are added by subsequent refinement steps. Skipping the details, this process corresponds to a partition of the domains $\mathbf{\Sigma}$ and **S** in the following way. Let

$$\mathbf{\Sigma}^0 := [0, 2]^2 \backslash [0, 1)^2, \ \ \mathbf{\Sigma}^m := 2^{-m}\mathbf{\Sigma}^0, \ \ \mathbf{S}^m := \mathbf{\Sigma}^m \times \mathbb{Z}_n, \ \ m \in \mathbb{N}_0 \,,$$

then

$$\mathbf{\Sigma} = \bigcup_{m \in \mathbb{N}} \mathbf{\Sigma}^m \cup \mathbf{0}, \quad \mathbf{S} = \bigcup_{m \in \mathbb{N}} \mathbf{S}^m \cup \mathbf{0}^{\mathrm{c}},$$

see Figure 5. Splines $\mathbf{x} \in C_0^k(\mathbf{S}, \mathbb{R}^d)$ are partitioned accordingly. For $m \in \mathbb{N}$ and $j \in \mathbb{Z}_n$, the *segment* $\mathbf{x}_j^m$ is defined by

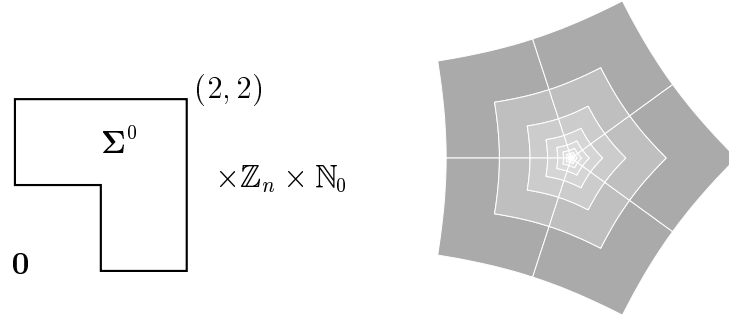$$\mathbf{x}_j^m : \mathbf{\Sigma}^0 \ni \boldsymbol{\sigma} \mapsto \mathbf{x}_j\big(2^{-m}\boldsymbol{\sigma}\big),$$

Figure 5: (*left*) Domain $\mathbf{S} \backslash \mathbf{0}^c$ for (*right*) the union $\mathbf{x} \backslash \mathbf{x}^c$ of spline rings.

and the *spline ring* $\mathbf{x}^m$ is defined by

$$\mathbf{x}^m : \mathbf{S}^0 \ni \mathbf{s} \mapsto \mathbf{x}(2^{-m}\mathbf{s}),$$

where we used the convention that a scalar factor applies only to the continuous variables of $\mathbf{s}$,

$$a\mathbf{s} = a(s, t, j) := (as, at, j), \quad a \in \mathbb{R}.$$

The space of all C^k-spline rings is denoted by

$$C^k(\mathbf{S}^0, \mathbb{R}^d).$$

The segment $\mathbf{x}_j^m$ corresponds to the restriction of the patch $\mathbf{x}_j$ to the set $\mathbf{\Sigma}^m$, and the spline ring $\mathbf{x}^m$ corresponds to the restriction of the spline $\mathbf{x}$ to the set $\mathbf{S}^m$, i.e.,

$$\mathbf{x}_j^m(\mathbf{\Sigma}^0) = \mathbf{x}_j(\mathbf{\Sigma}^m), \quad \mathbf{x}^m(\mathbf{S}^0) = \mathbf{x}(\mathbf{S}^m),$$

where re-scaling facilitates the use of a common domain for all m. This implies

$$\mathbf{x}_j(\mathbf{\Sigma}) = \bigcup_{m \in \mathbb{N}} \mathbf{x}_j^m(\mathbf{\Sigma}^0) \cup \mathbf{x}^c, \quad \mathbf{x}(\mathbf{S}) = \bigcup_{m \in \mathbb{N}} \mathbf{x}^m(\mathbf{S}^0) \cup \mathbf{x}^c.$$

The partition of a spline into spline rings and segments leads to the notion of subdivision. It refers to a special way of representing splines rather than to a new class of objects.

Definition 3.1 $\mathbf{x} \in C_0^k(\mathbf{S}, \mathbb{R}^d)$ *represented as*

$$\mathbf{x} : \mathbf{S} \ni \mathbf{s} \mapsto \begin{cases} \mathbf{x}^m(2^m\mathbf{s}) & \text{if} \quad \mathbf{s} \in \mathbf{S}^m \\ \mathbf{x}^c & \text{if} \quad \mathbf{s} = \mathbf{0}^c \end{cases}$$

is called a spline in subdivision form. *For $d = 3$, $\mathbf{x}$ is also called a* subdivision surface.

8

Expressing a spline in subdivision form is a straightforward segmentation process. This point of view becomes relevant if we proceed in the opposite direction and assume that the sequence of spline rings $\mathbf{x}^m$ is generated iteratively by some algorithm. Then the task is to analyze properties of the spline obtained by gluing all these pieces together. The following lemma characterizes the relation between spline rings and splines.

Lemma 3.2 *A sequence $(\mathbf{x}^m)_m$ of spline rings constitutes a spline $\mathbf{x} \in C_0^k(\mathbf{S}, \mathbb{R}^d)$ if and only if*

- *all segments are k-times continuously differentiable,*

$$\mathbf{x}_j^m \in C^k(\mathbf{\Sigma}^0, \mathbb{R}^d), \tag{5}$$

- *all pairs of neighboring segments $\mathbf{x}_j^m, \mathbf{x}_{j+1}^m$ satisfy*

$$\partial_s^\nu \mathbf{x}_j^m(0, 1 + u) = (-1)^\nu \partial_t^\nu \mathbf{x}_{j+1}^m(1 + u, 0), \quad u \in U, \tag{6}$$

- *all pairs of consecutive segments $\mathbf{x}_j^m$, $\mathbf{x}_j^{m+1}$ satisfy*

$$
\begin{aligned}
\partial_s^\nu \mathbf{x}_j^m(1, u) &= 2^\nu \partial_s^\nu \mathbf{x}_j^{m+1}(2, 2u) \\
\partial_t^\nu \mathbf{x}_j^m(u, 1) &= 2^\nu \partial_t^\nu \mathbf{x}_j^{m+1}(2u, 2), \quad u \in U,
\end{aligned} \tag{7}
$$

- *there exists $\mathbf{x}^c \in \mathbb{R}^d$ such that for any sequence $\mathbf{s}^m \in \mathbf{S}^0$*

$$\mathbf{x}^c = \lim_{m \to \infty} \mathbf{x}^m(\mathbf{s}^m). \tag{8}$$

We omit the details of the proof, which essentially reduces to an application of the chain rule. The following theorem summarizes conditions for normal continuity and single-sheetedness.

Theorem 3.3 *Let $\mathbf{x}^m$ be a sequence of spline rings satisfying all conditions of Lemma 3.2 and $\mathbf{x}$ the corresponding spline. Then*

- $\mathbf{x}$ *is normal continuous if and only if there exists $\mathbf{n}^c \in S^2$ such that for any sequence $\mathbf{s}^m \in \mathbf{S}^0$*

$$\mathbf{n}^c = \lim_{m \to \infty} \mathbf{n}^m(\mathbf{s}^m),$$

  where the spline rings of the Gauss map $\mathbf{n}$ are denoted by $\mathbf{n}^m$.

- $\mathbf{x}$ *is C_1^k, if and only if it is normal continuous and if there exists $m_0 \in \mathbb{N}$ such that*

$$\mathbf{n}^c \cdot \mathbf{n}^m > 0 \text{ for all } m \geq m_0, \text{ and}$$

the planar spline ring $\boldsymbol{\xi}_{m_0} := (\mathbf{x}_{m_0} - \mathbf{x}^c) \cdot \mathbf{T}^c$ corresponding to the projection $\boldsymbol{\xi}$ as defined in (2) is injective on the outer boundary of its domain

$$\partial_+ \mathbf{S}^0 := \{(s, t, j) \in \mathbf{S}^0 : \max(s, t) = 2\}.$$

While the proof of the first part is straightforward, the second part is nontrivial and requires techniques of differential topology. For details, we refer to [78].

All subdivision algorithms currently in use and a large class of generalizations are characterized by the fact that all spline rings generated by them lie in a common space which is the d-fold Cartesian product of a finite-dimensional space of real-valued functions. For instance, for the Doo-Sabin algorithm as described in Section 7, the spline rings are C^1 and consist of n segments of three biquadratic pieces each. The dimension of this space is therefore $9dn$. In general,

$$G := [g_0, \ldots, g_{\bar{\ell}}], \quad g_\ell \in C^k(\mathbf{S}^0, \mathbb{R}), \ \ell = 0, \ldots, \bar{\ell},$$

is a row-vector of scalar-valued spline rings and we assume that they form a partition of unity,

$$\sum_{\ell=0}^{\bar{\ell}} g_\ell(\mathbf{s}) = 1, \quad \mathbf{s} \in \mathbf{S}^0. \tag{9}$$

The spline space spanned by these functions is denoted

$$C^k(\mathbf{S}^0, \mathbb{R}^d, G) := \left\{ \sum_{\ell=0}^{\bar{\ell}} g_\ell \mathbf{q}_\ell : \mathbf{q}_\ell \in \mathbb{R}^d \right\} \subset C^k(\mathbf{S}^0, \mathbb{R}),$$

and G is called the *generating system* of $C^k(\mathbf{S}^0, \mathbb{R}^d, G)$. In many applications, G is linearly independent. This is explicitly not assumed here so that the analysis covers cases like generalized box spline subdivision or matrix subdivision schemes.

$C^k(\mathbf{S}^0, \mathbb{R}^d, G)$ is a linear function space of dimension $\leq d(\bar{\ell}+1)$. We endow it with the max-norm

$$\|\mathbf{x}^m\|_\infty := \max_{\mathbf{s} \in \mathbf{S}^0} |\mathbf{x}^m(\mathbf{s})|,$$

where $|\cdot|$ denotes the Euclidean norm in $\mathbb{R}^d$. Limits of sequences of spline rings are always understood with respect to this norm. The coefficients $\mathbf{q}_\ell^m \in \mathbb{R}^d$ of a spline ring

$$\mathbf{x}^m = \sum_{\ell=0}^{\bar{\ell}} g_\ell \mathbf{q}_\ell^m$$

are its *control points*. Collecting them in an $((\bar{\ell}+1) \times d)$-matrix $\mathbf{Q}^m := [\mathbf{q}_0^m; \ldots; \mathbf{q}_{\bar{\ell}}^m]$, we obtain

$$\mathbf{x}^m(\mathbf{s}) = \mathbf{x}_j^m(\boldsymbol{\sigma}) = G(\mathbf{s})\mathbf{Q}^m, \quad \mathbf{s} = (\boldsymbol{\sigma}, j) \in \mathbf{S}^0,$$

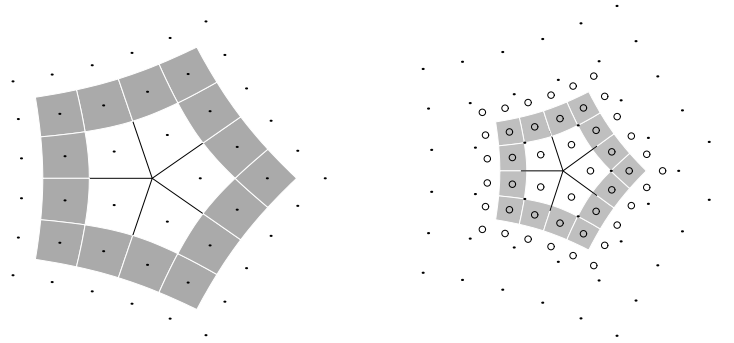or, omitting arguments, simply $\mathbf{x}^m = G\mathbf{Q}^m$.

Figure 6: (*left*) Control points **Q** (dots) and (*right*) refined control points $A\mathbf{Q}$ (∘) for Doo-Sabin subdivision [24]. The corresponding spline rings are shaded grey.

Bibliographic Notes.

- The idea of representing a subdivision surface as a union of spline rings dates back to [71, 73]. Early attempts to analyze smoothness [3, 4] were based on investigating sequences of finer and finer meshes converging to the subdivision surface. This approach, however, ultimately fails to capture important aspects of smoothness.

- Examples of subdivision surfaces which are not generated by a finite set of functions are, for instance, variational subdivision [41, 43] or schemes based on geometrical procedures as in [32].

4 Subdivision algorithms

From an abstract point of view, a subdivision algorithm is a rule to compute sequences of spline rings from an initial set of control points. Here, we focus on the following special case: a (linear stationary) *subdivision algorithm* (A, G) is characterized by a square matrix A with all rows summing to 1 and a generating system G of according dimension. For a given set **Q** of control points, also referred to as *initial data*, the sequence of spline rings is computed by iterated application of the matrix A,

$$\mathbf{Q}^m := A^m \mathbf{Q}, \quad \mathbf{x}^m = G A^m \mathbf{Q}.$$

Since the rows of A, as well as the functions in G, sum to 1, the representation of the spline rings x^m is affine invariant. That is, applying an affine transformation to the initial control points **Q** is equivalent to applying this transformation to the spline rings $\mathbf{x}^m$, and hence to the complete spline **x**.

The analysis of a subdivision algorithm can be split into three parts. First, the smoothness of the generating system has to be determined by verifying (5) and (6). Second, the contact conditions (7) between neighboring and consecutive segments

have to be verified. Typically, this task is readily accomplished. Third, and this is the focus of this work, continuity and smoothness properties at the center have to be determined.

We start with continuity as defined by (8). Since the rows of A sum to one, $\lambda_0 := 1$ is the eigenvalue corresponding to the eigenvector $e := [1, \ldots, 1]^{\mathrm{T}}$, i.e., $Ae = e$. To ensure (8), i.e.

$$\lim_{m \to \infty} \mathbf{x}^m = \mathbf{x}^c,$$

it seems natural to demand that this eigenvalue be dominant. However, in general, this is by no means necessary. The reason for this is that the generating system need not be linearly independent. For example, assume that A has eigenvalues $\lambda_0 = 1$, $\lambda = 2$ and $\mu = 1/2$ corresponding to the eigenvectors e, v and w, respectively. Let $\mathbf{Q} = v\mathbf{p} + e\mathbf{q} + w\mathbf{r}$ for some points $\mathbf{p}, \mathbf{q}, \mathbf{r} \in \mathbb{R}^d \setminus \{\mathbf{0}\}$. Then $\mathbf{Q}^m = A^m \mathbf{Q} = 2^m v\mathbf{p} + e\mathbf{q} + 2^{-m} w\mathbf{r}$ is certainly divergent. But if v happens to be annihilated by G, i.e. $Gv = 0$, then $\mathbf{x}^m = G\mathbf{Q}^m = \mathbf{q} + 2^{-m} Gw\mathbf{r} \to \mathbf{q} =: \mathbf{x}^c$ is convergent. We say that v is an *ineffective eigenvector*.

This shows that, in general, it is not possible to relate spectral properties of A to smoothness properties of the generated surfaces in a straightforward way. To address this issue in a consistent fashion, we proceed as follows. We define the linear spaces

$$N := \{v \in \mathbb{R}^{\ell+1} : Gv = 0\}, \quad M_A := \bigcap_{m \in \mathbb{N}} A^m N.$$

That is, M_A consists of all vectors that do not escape the nullspace of G when A is applied. Further, two matrices $A, \tilde{A}$ are called *G-equivalent* if they generate identical sequences of control points, i.e., if $GA^m = G\tilde{A}^m$ for all $m \in \mathbb{N}_0$. Then the following holds:

Lemma 4.1 (Removal of ineffective eigenvectors) *a) For given $(\tilde{A}, G)$, let $\Pi_0 : \mathbb{R}^{\ell+1} \to M_{\tilde{A}}$ be a projection on $M_{\tilde{A}}$ with $\Pi_0 e = 0$, and $\Pi_1 := \mathrm{Id} - \Pi_0$ its complement. Then the matrices $A := \Pi_1 \tilde{A}$ and $\tilde{A}$ are G-equivalent, and $M_A = \{0\}$.*

b) If $M_A = \{0\}$, then A does not have ineffective eigenvectors. That is, if $Av = \lambda v \neq 0$ then $Gv \neq 0$.

Proof a) Since $Ge = 1$ by (9), we have $e \notin M_{\tilde{A}}$, and a projection of the desired form exists. By definition, $AM_A = M_A$ and $\tilde{A}M_{\tilde{A}} = M_{\tilde{A}}$. Hence,

$$\tilde{A}(M_{\tilde{A}} + M_A) = M_{\tilde{A}} + \Pi_0 \tilde{A} M_A + \Pi_1 \tilde{A} M_A = M_{\tilde{A}} + M_A.$$

Since $M_{\tilde{A}}$ is the largest $\tilde{A}$-invariant subspace of N, $M_A \subset M_{\tilde{A}}$. Further $M_{\tilde{A}} \subset \ker \tilde{A} \subset \ker A$ and $AM_A = M_A$ so that $M_A = \{0\}$. Finally, $Ae = \Pi_1 \tilde{A} e = e$. It remains to show that A and $\tilde{A}$ are equivalent. To this end, we consider $G(A^m - \tilde{A}^m) = G\big((\tilde{A} - \Pi_0 \tilde{A})^m - \tilde{A}^m\big) =: G\Delta$. The matrix Δ is the sum of products of matrices $\tilde{A}$ and Π_0 all of which include the factor Π_0. With $\tilde{A}\Pi_0 = \Pi_0 \tilde{A}\Pi_0$, it is clear that Δ can be represented in the form $\Delta = \Pi_0 \Delta'$. Therefore $G(A^m - \tilde{A}^m) = G\Pi_0 \Delta' = \mathbf{0}$.

b) If $Av = \lambda v \neq 0$, then for all $m \in \mathbb{N}$ we have $Gv = \lambda^{-m} GA^m v = 0$. Hence, $A^m v \in N$ and $v \in M_A$ contradicting $M_A = \{0\}$. $\qquad\square$

The property $M_A = \{0\}$, which is trivial for linearly independent G, can now be assumed for the general setting without loss of generality. The following theorem crucially depends on this property.

Theorem 4.2 *Let (A, G) be a subdivision algorithm with $M_A = \{0\}$. Then the continuity condition*

$$\mathbf{x}^{\mathrm{c}} = \lim_{m \to \infty} \mathbf{x}^m$$

is satisfied for any set $\mathbf{Q}$ of initial data if and only if the eigenvalue $\lambda_0 = 1$ of A is strictly dominant, i.e., if $|\lambda| < 1$ for all other eigenvalues λ of A.

Proof Let $\lambda_0 = 1$ be strictly dominant. With $\tilde{e}^{\mathrm{T}} = \tilde{e}^{\mathrm{T}}A$ the left eigenvector to λ_0 normalized by $\tilde{e}^{\mathrm{T}}e = 1$, we can decompose $\mathbf{Q}$ in the form $\mathbf{Q} = e\tilde{e}^{\mathrm{T}}\mathbf{Q} + \mathbf{R}$, where $\mathbf{R}$ is a linear combination of generalized eigenvectors of A corresponding to eigenvalues λ_i with $|\lambda_i| < r$ for some constant $r < 1$. Hence, using $Ge = 1$, we obtain convergence according to

$$\mathbf{x}^m = GA^m\mathbf{Q} = \tilde{e}^{\mathrm{T}}\mathbf{Q} + o(r^m) \to \tilde{e}^{\mathrm{T}}\mathbf{Q} =: \mathbf{x}^{\mathrm{c}}.$$

If $\lambda_0 = 1$ is not strictly dominant, we have to distinguish two cases. If $\lambda_0 = 1$ has geometric multiplicity 1, but algebraic multiplicity > 1, then there exists a generalized eigenvector v with $Av = v + e$. We set $\mathbf{q} := [1, \ldots, 1]$ and $\mathbf{Q} := v\mathbf{q}$ to obtain the divergent sequence

$$\mathbf{x}^m = GA^m\mathbf{Q} = GA^m v\mathbf{q} = G(v + me)\mathbf{q} = G\mathbf{Q} + m\mathbf{q}.$$

Otherwise, there exists an eigenvector v, which is linearly independent of e, to an eigenvalue λ with $|\lambda| \geq 1$. We set $\mathbf{q} := [1, \ldots, 1]$, $\mathbf{Q} := \mathrm{Re}\, v\mathbf{q}$, and $\lambda =: |\lambda|e^{it}$ to obtain

$$\mathbf{x}^m = GA^m\mathbf{Q} = |\lambda|^m \mathrm{Re}(e^{imt}Gv\mathbf{q}).$$

Since $Gv \neq 0$, this expression can converge to a constant $\mathbf{x}^{\mathrm{c}}$ only if $|\lambda| = 1$ and $t = 0$, i.e., if the eigenvalue $\lambda = \lambda_0 = 1$ is at least double, and if $Gv =: \alpha \in \mathbb{R}$ is constant. In this case, $v' := \alpha e - v$ is an ineffective eigenvector because $Av' = v' \neq 0$ and $Gv' = G(\alpha e - v) = 0$ contradicting Lemma 4.1. $\qquad\square$

The results obtained so far suggest confining our considerations to subdivision schemes with $M_A = \{0\}$ and a strictly dominant eigenvalue $\lambda_0 = 1$. The next definition accounts for that.

Definition 4.3 *Let (A, G) be a subdivision scheme with the following properties:*

- *The generating system is C^k, i.e., $G \in C^k(\mathbf{S}^0, \mathbb{R}^{\bar{\ell}+1})$.*

- *The conditions (7) are satisfied.*

- *A has no ineffective eigenvectors, i.e., $M_A = \{0\}$.*

13

- *The eigenvalue $\lambda_0 = 1$ to the eigenvector $e = Ae$ is strictly dominant.*

Then (A, G) *is called a* C_0^k*-scheme, and A is called the* subdivision matrix.

We recall our convention that the superscript k refers to the smoothness of the parametrization, while the subscript 0 indicates continuity at the center. We summarize our previous findings in the following theorem:

Theorem 4.4 *Let (A, G) be a C_0^k-scheme and $\tilde{e} = \tilde{e}A$ the dominant left eigenvector normalized by $\tilde{e}e = 1$. Then, for any $\mathbf{Q}$, the spline rings $\mathbf{x}^m := GA^m\mathbf{Q}$ together with the center $\mathbf{x}^c := \tilde{e}\mathbf{Q}$ constitute a C_0^k-spline.*

We continue by defining B-spline-like functions for subdivision algorithms. Denote the unit vectors in $\mathbb{R}^{\bar{\ell}+1}$ by $e_0, \ldots, e_{\bar{\ell}}$, and define the row-vector $B = [b_0, \ldots, b_{\bar{\ell}}]$ of real-valued splines $b_\ell \in C_0^k(\mathbf{S}, \mathbb{R})$ by

$$b_\ell(\mathbf{s}) := \begin{cases} G(2^m\mathbf{s})A^m e_\ell & \text{if} \quad \mathbf{s} \in \mathbf{S}^m \\ \tilde{e}e_\ell & \text{if} \quad \mathbf{s} = \mathbf{0}^c. \end{cases} \tag{10}$$

Then, by linearity of subdivision, the relation between arbitrary initial data $\mathbf{Q}$ and the corresponding spline $\mathbf{x}$ can simply be written as

$$\mathbf{x} = B\mathbf{Q}. \tag{11}$$

Let us briefly discuss some properties of the functions in B. They

- *span the the space of splines* generated by the subdivision algorithm (A, G).

- form a *partition of unity* since

$$\sum_{\ell=0}^{\bar{\ell}} b_\ell(\mathbf{s}) = \begin{cases} G(2^m\mathbf{s})A^m e = G(2^m\mathbf{s})e = 1 & \text{if} \quad \mathbf{s} \in \mathbf{S}^m \\ \tilde{e}e = 1 & \text{if} \quad \mathbf{s} = \mathbf{0}^c. \end{cases}$$

- are *linearly independent*, if the generating system G is linearly independent. To show this, it suffices to consider the initial spline ring $\mathbf{x}_0 = G\mathbf{Q} = G\mathbf{Q}_0$ which, for linearly independent G, vanishes if and only if $\mathbf{Q} = \mathbf{0}$.

- satisfy the *scaling relation*

$$B(2^{-m}\mathbf{s}) = B(\mathbf{s})A^m, \quad \mathbf{s} \in \mathbf{S}, \ m \in \mathbb{N}_0.$$

This can be proven as follows. For $\mathbf{s} \in \mathbf{S}^{m'}$, (10) yields $B(\mathbf{s}) = G(2^{m'}\mathbf{s})A^{m'}$. For $m \in \mathbb{N}_0$, it is $2^{-m}\mathbf{s} \in \mathbf{S}^{m+m'}$, and accordingly $B(2^{-m}\mathbf{s}) = G(2^{m'}\mathbf{s})A^{m+m'}$. Comparison of the two equations, which hold for any $m' \in \mathbb{N}$, verifies the claim.

14

The functions in B are important for many applications like solving interpolation or approximation problems for subdivision surfaces. In view of (11), the similarity with B-splines in the standard setting is evident. The only conceptional differences concern possible linear dependencies and a lack of parametric smoothness at the center. We will focus on geometric smoothness properties in the next sections.

Bibliographic Notes.

- Dominance of the eigenvector $\lambda_0 = 1$ was always considered a necessary condition for subdivision algorithms. The intriguing phenomenon of ineffective eigenvectors was first discussed in [77]. An example which shows that requiring linear independence of the generating system implies a loss of generality can be found in [78].

- A constructive procedure to efficiently compute a subdivision matrix A from a given matrix $\tilde{A}$ can be found in [78].

- The representation (11) of a subdivision surface as a finite linear combination of control points $\mathbf{q}_\ell$ and functions b_ℓ is most useful for computational purposes. For instance, it was used in [19] to compute subdivision surfaces which minimize a certain fairness functional while interpolating a given set of points.

- There exists a well-developed theory for the analysis of subdivision curves and surfaces when the domain manifold $\mathbf{S}$ is homeomorphic to the plane, see for instance [10, 28, 44, 53, 54].

- The linear independence and (lack of) local linear independence of subdivision functions has been analyzed in detail in [65].

5 C_1^k-schemes and the characteristic map

In this section, we derive necessary and sufficient conditions for normal continuity and single-sheetedness of subdivision surfaces. As already mentioned above, the spectrum of A is crucial for the properties of a subdivision scheme. We sort the eigenvalues λ_i of A in descending order,

$$1 = \lambda_0 > |\lambda_1| \geq |\lambda_2| \geq \cdots |\lambda_{\bar{\ell}}|.$$

To simplify the exposition, we focus on a subclass of subdivision algorithms that covers all cases of practical relevance.

Definition 5.1 A C_0^k-scheme (A, G) according to Definition 4.3 is called a standard scheme, if $k \geq 1$, and

- A has a double subdominant eigenvalue λ, i.e.,

$$1 > \lambda := \lambda_1 = \lambda_2 > |\lambda_3|,$$

- *there exist two linearly independent eigenvectors v_1, v_2 to λ, i.e.,*

$$A\mathbf{v} = \lambda\mathbf{v}, \quad \mathbf{v} = [v_1, v_2].$$

Such an eigenstructure is not really special, but typical for schemes with certain natural symmetry properties, as discussed in Section 6. Let $A =: VJV^{-1}$ denote the Jordan decomposition of the subdivision matrix of a standard scheme. Then $V = [e, v_1, v_2, \tilde{V}]$ and $J = \mathrm{diag}(1, \lambda, \lambda, \tilde{J})$. We define the *eigencoefficients* $\mathbf{P} = [\mathbf{p}_0; \ldots; \mathbf{p}_{\bar{\ell}}]$ and the *eigenfunctions* $F = [f_0, \ldots, f_{\bar{\ell}}]$ by

$$\mathbf{P} := V^{-1}\mathbf{Q}, \quad F := GV.$$

With $\mathbf{p}_0 = \tilde{e}^{\mathrm{T}}\mathbf{Q} = \mathbf{x}^{\mathrm{c}}$ the center and $f_0 = Ge = 1$ the 1-function we obtain the representation

$$\mathbf{x}^m = GA^m\mathbf{Q} = FJ^m\mathbf{P} = \mathbf{x}^{\mathrm{c}} + \lambda^m(f_1\mathbf{p}_1 + f_2\mathbf{p}_2) + o(\lambda^m).$$

To efficiently deal with such *asymptotic expansions*, we introduce an equivalence relation for sequences of functions with coinciding leading terms. We write

$$a^m \overset{c^m}{=} b^m \quad \text{iff} \quad a^m - b^m = o(c^m),$$

where $o(c^m)/c^m$ converges uniformly to zero as $m \to \infty$. For example, $a^m \overset{1}{=} a$ means that a^m converges to a. For vector-valued expressions, the equivalence relation is understood component-wise. For simplicity, $\overset{c^m}{=}$ is mostly replaced by the symbol $\doteq$ with the understanding that the dot refers to the lowest order term specified explicitly on the right hand side of a relation. Hence, the expansion of the sequence of spline rings above now simply reads $\mathbf{x}^m \doteq \mathbf{x}^{\mathrm{c}} + \lambda^m(f_1\mathbf{p}_1 + f_2\mathbf{p}_2)$, meaning that the omitted remainder term decays faster than λ^m. In the following, the two-dimensional spline ring built from the subdominant eigenfunctions f_1, f_2 plays a central role.

Definition 5.2 *For a standard scheme (A, G) with subdominant eigenvectors $\mathbf{v} = [v_1, v_2]$ and eigenfunctions $F = [1, f_1, f_2, \ldots, f_{\bar{\ell}}]$ the* characteristic map *is defined by*

$$\boldsymbol{\psi} := G\mathbf{v} = [f_1, f_2] \in C^k(\mathbf{S}^0, \mathbb{R}^2, G).$$

With this definition, the sequence of spline rings becomes

$$\mathbf{x}^m \doteq \mathbf{x}^{\mathrm{c}} + \lambda^m \boldsymbol{\psi}[\mathbf{p}_1; \mathbf{p}_2].$$

Convergence towards the center $\mathbf{x}^{\mathrm{c}}$ is evident. In order to compute normal vectors, we define the cross product of vectors in $\mathbb{R}^3$ as usual, and for vectors in $\mathbb{R}^2$ as the real number $\boldsymbol{\alpha} \times \boldsymbol{\beta} := \det(\boldsymbol{\alpha}, \boldsymbol{\beta})$. Accordingly, for spline rings in $\mathbb{R}^2$ or $\mathbb{R}^3$, we define the differential operator ${}^{\times}\!D := \partial_s \times \partial_t$ and obtain

$$
{}^{\times}\!D\mathbf{x}^m = \partial_s\mathbf{x}^m \times \partial_t\mathbf{x}^m \doteq \lambda^{2m} \, {}^{\times}\!D\boldsymbol{\psi} \, (\mathbf{p}_1 \times \mathbf{p}_2),
$$

16

where, by definition,

$$^\times\!D\boldsymbol{\psi} = \partial_s f_1 \, \partial_t f_2 - \partial_t f_1 \, \partial_s f_2$$

is the Jacobian determinant of the characteristic map. It is easily shown that $^\times\!D\boldsymbol{\psi} \in C^{k-1}(\mathbf{S}^0, \mathbb{R}^2)$ if $\boldsymbol{\psi} \in C^k(\mathbf{S}^0, \mathbb{R}^2)$. In order to distinguish degenerate cases, we say that the initial data $\mathbf{Q}$ are *generic*, if any three of the eigencoefficients $\mathbf{p}_1, \ldots, \mathbf{p}_{\bar{\ell}}$ are linearly independent. In this section, it would be sufficient to demand only $\mathbf{p}_1 \times \mathbf{p}_2 \neq \mathbf{0}$; the generality of the definition anticipates the requirements in the next sections. We say that a subdivision scheme is *normal continuous* or *single-sheeted*, if so are all surfaces generated from generic initial data.

Theorem 5.3 *A standard scheme is*

- *normal continuous with central normal*

$$\mathbf{n}^c = \operatorname{sign}(^\times\!D\boldsymbol{\psi}) \frac{\mathbf{p}_1 \times \mathbf{p}_2}{|\mathbf{p}_1 \times \mathbf{p}_2|},$$

  if the characteristic map is regular, i.e., if $^\times\!D\boldsymbol{\psi} \neq 0$.

- *not normal continuous, if $^\times\!D\boldsymbol{\psi}$ changes sign.*

Proof The first part of the statement follows immediately from $\mathbf{n}^m := {}^\times\!D\mathbf{x}^m / |{}^\times\!D\mathbf{x}^m|$ and the observation that $1/{}^\times\!D\boldsymbol{\psi}$ is continuous, hence uniformly bounded, on the compact domain $\mathbf{S}^0$. To proof the second part, let us assume that $^\times\!D\boldsymbol{\psi}(\mathbf{s}_1)\,{}^\times\!D\boldsymbol{\psi}(\mathbf{s}_2) < 0$ for some arguments $\mathbf{s}_1, \mathbf{s}_2 \in \mathbf{S}^0$. Here, we obtain

$$\mathbf{n}^m(\mathbf{s}_i) \doteq \operatorname{sign}(^\times\!D\boldsymbol{\psi}(\mathbf{s}_i)) \frac{\mathbf{p}_1 \times \mathbf{p}_2}{|\mathbf{p}_1 \times \mathbf{p}_2|}, \quad i \in \{1, 2\},$$

and see that $\mathbf{n}^m$ cannot converge to a constant limit since $|\mathbf{n}^m(\mathbf{s}_1) - \mathbf{n}^m(\mathbf{s}_2)| \doteq 2$. $\quad\square$

The conditions of this theorem are almost comprehensive. Only the exceptional case, where $^\times\!D\boldsymbol{\psi}$ has zeros without changing sign remains open. Here, the behavior of $^\times\!D\mathbf{x}^m$ depends on higher order eigencoefficients and cannot be determined a priori. Now, the issue of single-sheetedness has to be addressed, and again, the characteristic map provides necessary and sufficient conditions.

Theorem 5.4 *A standard C_0^k-scheme with a regular characteristic map $\boldsymbol{\psi}$ is*

- *single-sheeted and moreover C_1^k, if $\boldsymbol{\psi}$ is injective.*

- *not single sheeted, if $\boldsymbol{\psi}$ restricted to the interior of $\mathbf{S}^0$ is not injective.*

17

Proof Let $\boldsymbol{\psi}$ be regular and injective. Then we know that $\mathbf{x}$ is normal continuous with $\mathbf{n}^m \doteq \mathbf{n}^c = \mathrm{sign}(^{\times}\!D\boldsymbol{\psi}(\mathbf{s}_i))(\mathbf{p}_1 \times \mathbf{p}_2)/|\mathbf{p}_1 \times \mathbf{p}_2|$. Hence, $\mathbf{n}^c \cdot \mathbf{n}^m \doteq 1$, and in particular $\mathbf{n}^c \cdot \mathbf{n}^m > 0$ for m sufficiently large. Next, we consider a rescaled sequence of projections of spline rings,

$$\tilde{\boldsymbol{\xi}}^m := \lambda^{-m}\boldsymbol{\xi}^m \doteq \boldsymbol{\psi}L, \quad L := [\mathbf{p}_1; \mathbf{p}_2] \cdot \mathbf{T}^c.$$

For generic initial data, $\boldsymbol{\psi}L$ is injective because the (2×2)-matrix L has full rank. Since the set of regular injective mappings is open with respect to the C^1-norm, we conclude that $\tilde{\boldsymbol{\xi}}^m$ and eventually $\boldsymbol{\xi}^m$ is injective for m sufficiently large. Thus, all conditions of Theorem 3.3 are fulfilled, and $\mathbf{x}$ is C_1^k. Similar arguments show that also non-injectivity of $\boldsymbol{\psi}$ at interior points is inherited by $\tilde{\boldsymbol{\xi}}^m$ and $\boldsymbol{\xi}^m$. $\qquad\square$

Again, the theorem is almost comprehensive. Only the exceptional case, when $\boldsymbol{\psi}$ restricted to the boundary of its domain is not injective, remains open. Theorems 5.3 and 5.4 suggest to focus on standard schemes with a regular and injective characteristic map. The following definition accounts for that observation.

Definition 5.5 *A standard C_0^k-scheme (A, G) with a characteristic map $\boldsymbol{\psi}$ that is regular and injective is called a* standard C_1^k-scheme. *$\boldsymbol{\psi}$ is called* normalized *if*

$$\boldsymbol{\psi}(2, 2, 0) = (1, 0) \quad and \quad {}^{\times}\!D\boldsymbol{\psi} > 0.$$

As we have shown, C_1^k-schemes generate C_1^k-splines from generic initial data. The notion of normalization is introduced to select from the variety of possible characteristic maps a special class of representatives which is convenient for the forthcoming considerations. We prepare our discussion of that issue by the following observation. For initial data $\mathbf{Q} := [v_1, v_2]$ the corresponding two-dimensional spline is $\mathbf{x} = B\mathbf{v} \in C_0^k(\mathbf{S}, \mathbb{R}^2)$, where the spline rings are just scaled copies of the characteristic map, $\mathbf{x}^m = \lambda^m\boldsymbol{\psi}$. By (7), this implies for the segments $\boldsymbol{\psi}_j$

$$\boldsymbol{\psi}_j(1, u) = \lambda\boldsymbol{\psi}_j(2, 2u)$$
$$\boldsymbol{\psi}_j(u, 1) = \lambda\boldsymbol{\psi}_j(2u, 2), \tag{12}$$

and in general

$$\partial_s^\nu \boldsymbol{\psi}_j(1, u) = \lambda\, 2^\nu \partial_s^\nu \boldsymbol{\psi}(2, 2u)$$
$$\partial_t^\nu \boldsymbol{\psi}_j(u, 1) = \lambda\, 2^\nu \partial_t^\nu \boldsymbol{\psi}(2u, 2), \quad 0 \le \nu \le k. \tag{13}$$

Now, we can prove that normalization is always possible if the characteristic map is regular and injective.

Lemma 5.6 *Let $\tilde{\boldsymbol{\psi}} = F\tilde{\mathbf{v}}$ be the characteristic map of a standard C_1^k-scheme with $s := \mathrm{sign}\,\tilde{\boldsymbol{\psi}}(2, 2, 0)$ and $[a, b] := \tilde{\boldsymbol{\psi}}(2, 2, 0)$. Then $[a, b] \ne [0, 0]$, and*

$$\boldsymbol{\psi} := F\mathbf{v}, \quad \mathbf{v} := \tilde{\mathbf{v}}R, \quad R := \frac{1}{a^2 + b^2}\begin{bmatrix} a & -sb \\ b & sa \end{bmatrix}$$

defines a normalized characteristic map of the scheme.

18

Proof By (13) and injectivity, $\tilde{\boldsymbol{\psi}}(1,1,0) = \lambda\tilde{\boldsymbol{\psi}}(2,2,0) \neq \tilde{\boldsymbol{\psi}}(2,2,0)$. Hence, $[a,b] \neq [0,0]$, and R is well defined. Since R has full rank, the columns of $\mathbf{v}$ are linearly independent eigenvectors of A to λ implying that $\boldsymbol{\psi} = F\mathbf{v} = \tilde{\boldsymbol{\psi}}R$ is a characteristic map as well as $\tilde{\boldsymbol{\psi}}$. In particular, $\boldsymbol{\psi}$ is regular and injective. We find $\boldsymbol{\psi}(2,2,0) = \tilde{\boldsymbol{\psi}}(2,2,0)R = [1,0]$, and

$$^x\!D\boldsymbol{\psi}(2,2,0) = {}^x\!D\tilde{\boldsymbol{\psi}}(2,2,0)\det R = \frac{|^x\!D\tilde{\boldsymbol{\psi}}(2,2,0)|}{a^2 + b^2} > 0.$$

Since $^x\!D\boldsymbol{\psi}$ is continuous and has no zeros, $^x\!D\boldsymbol{\psi} > 0$ follows showing that $\boldsymbol{\psi}$ is normalized. $\square$

Bibliographic Notes.

- As pointed out in [63], shift and flip invariance (see Section 6) of a C_1^k-scheme imply a double subdominant Jordan block. For instance, for $n = 3$, simplest subdivision [62] yields an 6-fold subdominant eigenvalue $\lambda_1 = 1/4$, with two Jordan blocks of size 2 and two Jordan blocks of size 1. Still, C_1^k-smoothness is guaranteed. The analysis of this more general setting is only slightly more difficult, but requires considerably complex notation. The standard case discussed here covers most algorithms currently in use.

- Complete lists of possible leading eigenvalues campatible with C_1^k-schemes are provided in [77, 98].

- The concept of the characteristic map was introduced in [73]. In some sense, it is related to the *natural configuration* defined in [92].

- In [73], it is shown that regularity and injectivity of the characteristic map are sufficient for smoothness. Necessity was proven in [63].

- An elegant computational way to verify regularity of the characteristic map even for non-polynomial schemes is described in [99].

6 Symmetry and Fourier analysis

We continue the analysis of schemes with standard symmetry properties. According to the partition of splines into segments, vectors $\mathbf{Q}$ of control points can typically be partitioned into blocks $\mathbf{Q} = [\mathbf{Q}_0; \ldots; \mathbf{Q}_{n-1}]$, where all blocks $\mathbf{Q}_j$ have equal structure and size $\tilde{\ell} := (\bar{\ell} + 1)/n$. If, as for the Catmull-Clark scheme, a central control point is common to all blocks, one can use n identical copies of it to achieve the desired structure. Shift invariance of a subdivision scheme refers to the fact that the shape of a subdivision surface does not depend on the special choice of the starting point

when indexing the blocks of a given set of initial data $\mathbf{Q}$. More precisely, with E the identity matrix of dimension $\tilde{\ell}$, let

$$S := \begin{bmatrix} 0 & 0 & \cdots & 0 & E \\ E & 0 & \cdots & 0 & 0 \\ & & \ddots & & \\ 0 & 0 & \cdots & E & 0 \end{bmatrix}$$

denote the n-block shift matrix. A subdivision scheme (A, G) is called *shift invariant*, if

$$AS = SA \quad \text{and} \quad G(\cdot, j) = G(\cdot, j+1)S, \quad j \in \mathbb{Z}_n.$$

In this case, for any $\mathbf{Q}$ and $\tilde{\mathbf{Q}} := S^k \mathbf{Q}$, the segments of the splines $\mathbf{x} := B\mathbf{Q}$ and $\tilde{\mathbf{x}} := B\tilde{\mathbf{Q}}$ differ, just as the blocks $\mathbf{Q}_j = \tilde{\mathbf{Q}}_{j+k}$ of the initial data, only by an index shift:

$$\mathbf{x}_j = G(\cdot, j)A^m \mathbf{Q} = G(\cdot, j+k)S^k A^m \mathbf{Q} = G(\cdot, j+k)A^m S^k \mathbf{Q} = \tilde{\mathbf{x}}_{j+k}.$$

Flip invariance of a subdivision scheme refers to the fact that the shape of a subdivision surface does not depend on the orientation when indexing a given set of initial control points $\mathbf{Q}$. More precisely, a subdivision scheme (A, G) is called *flip invariant*, if there exists a matrix R with $R = R^{-1}$ such that

$$AR = RA \quad \text{and} \quad G(s, t, j) = G(t, s, -j)R, \quad (s, t, j) \in \mathbf{S}^0. \tag{14}$$

In this case, for any $\mathbf{Q}$ and $\tilde{\mathbf{Q}} := R\mathbf{Q}$, the splines $\mathbf{x} := B\mathbf{Q}$ and $\tilde{\mathbf{x}} := B\tilde{\mathbf{Q}}$ differ only by a flip $(s, t, j) \to (t, s, -j)$ of arguments,

$$\mathbf{x}_j(s, t) = G(s, t, j)A^m \mathbf{Q} = G(t, s, -j)RA^m \mathbf{Q} = G(t, s, -j)A^m R\mathbf{Q} = \tilde{\mathbf{x}}_{-j}(t, s).$$

From now on, we focus on schemes which respect both invariance principles.

Definition 6.1 *A subdivision scheme is called* symmetric, *if it is both shift and flip invariant.*

Let us continue by discussing the implications of symmetry on the eigenstructure of A. $SA = AS$ implies a block-circulant structure for the subdivision matrix,

$$A = \begin{bmatrix} A_0 & A_{n-1} & \cdots & A_1 \\ A_1 & A_0 & \cdots & A_2 \\ \vdots & \vdots & \ddots & \vdots \\ A_{n-1} & A_{n-2} & \cdots & A_0 \end{bmatrix}.$$

The key tool for handling such matrices is the *Discrete Fourier Transform (DFT)*. With

$$w_n := \exp(2\pi i / n),$$

the primitive n-th root of unity we define the *Fourier block matrix* W as the Kronecker product of E and the Fourier matrix, i.e.

$$
W := (w_n^{-jk} E)_{j,k \in \mathbb{Z}_n} = \begin{bmatrix}
E & E & E & \cdots & E \\
E & w_n^{-1}E & w_n^{-2}E & \cdots & w_n^{1}E \\
E & w_n^{-2}E & w_n^{-4}E & \cdots & w_n^{2}E \\
\vdots & \vdots & \vdots & \ddots & \vdots \\
E & w_n^{1}E & w_n^{2}E & \cdots & w_n^{-1}E
\end{bmatrix}.
$$

It is easily verified by inspection that the inverse of W is given by

$$
W^{-1} = \frac{1}{n}\,(w_n^{+jk}E)_{j,k \in \mathbb{Z}_n} = \frac{1}{n}\,\overline{W}.
$$

The DFT of the matrix A is defined by $\hat{A} := WAW^{-1}$, and a standard computation shows that

$$
\hat{A} = \mathrm{diag}(\hat{A}_0, \ldots, \hat{A}_{n-1})
$$

is block diagonal with entries obtained by applying the Fourier matrix to the first block column of A,

$$
\begin{bmatrix} \hat{A}_0 \\ \vdots \\ \hat{A}_{n-1} \end{bmatrix} := W \begin{bmatrix} A_0 \\ \vdots \\ A_{n-1} \end{bmatrix}, \quad \text{that is} \quad \hat{A}_k := \sum_{j \in \mathbb{Z}_n} w_n^{-jk} A_j.
$$

By definition, A and $\hat{A}$ are similar, and in particular, they have equal eigenvalues. More precisely, if λ' is an eigenvalue of A, then there exists an index $k \in \mathbb{Z}_n$ such that λ' is an eigenvalue of $\hat{A}_k$. The set of all such indices is called the *Fourier index* of λ' and denoted

$$
\mathcal{F}(\lambda') := \{ k \in \mathbb{Z}_n : \det(\hat{A}_k - \lambda'E) = 0 \}.
$$

For the dominant eigenvalue $\lambda_0 = 1$ of A, we obtain $\mathcal{F}(1) = \{0\}$. Now we consider the double subdominant eigenvalue λ of a standard scheme. If $k \in \mathcal{F}(\lambda)$, then

$$
\det(\hat{A}_k - \lambda E) = \det(\hat{A}_{n-k} - \lambda E) = 0
$$

since λ is real and the diagonal blocks $\hat{A}_k$ and $\hat{A}_{n-k}$ are complex conjugate (unless $k = 0$ or $k = n - k$). Hence, the Fourier index of λ has the form $\mathcal{F} = \{k, n - k\}$ for some $k \in \mathbb{Z}_n$. If $\hat{A}_k \hat{v} = \lambda \hat{v}$, then the corresponding complex eigenvector of A is given by

$$
v = W^{-1} \begin{bmatrix} \delta_{0,k}\hat{v} \\ \delta_{1,k}\hat{v} \\ \vdots \\ \delta_{n-1,k}\hat{v} \end{bmatrix} = \frac{1}{n} \begin{bmatrix} w_n^{0}\hat{v} \\ w_n^{k}\hat{v} \\ \vdots \\ w_n^{(n-1)k}\hat{v} \end{bmatrix}. \tag{15}
$$

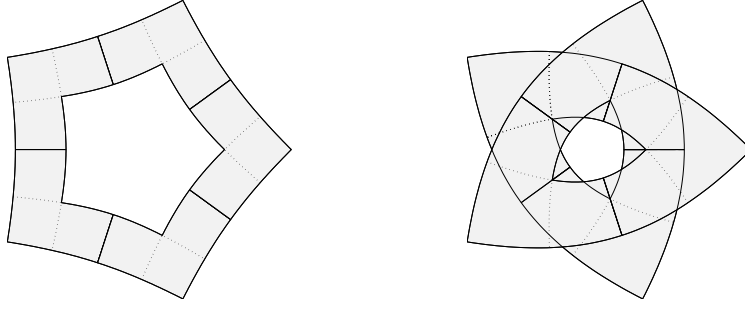The eigenfunction corresponding to v is just a complex version of the characteristic map ψ.

21

Figure 7: Characteristic map with Fourier index (*left*) $\mathcal{F}(\lambda) = \{1, n-1\}$ and (*right*) $\mathcal{F}(\lambda) = \{2, n-2\}$.

Definition 6.2 *Let v be the complex eigenvector of a symmetric standard C_1^k-scheme (A, G) to the subdominant eigenvalue λ as defined above. Then the* complex characteristic map *of the scheme is defined as the spline ring*

$$f := Gv \in C^k(\mathbf{S}^0, \mathbb{C}, G).$$

This definition is justified as follows: The real and imaginary part of v are the real eigenvectors v_1, v_2 as introduced in Definition 5.1. Hence,

$$f = G(v_1 + iv_2) = f_1 + if_2 \quad \text{and} \quad \boldsymbol{\psi} = G[v_1, v_2] = [\operatorname{Re} f, \operatorname{Im} f].$$

Further, with $^\times\!Df := \operatorname{Im}(\overline{\partial_s f}\,\partial_t f)$,

$$^\times\!Df = {}^\times\!D\boldsymbol{\psi}.$$

Due to the close relation between $\boldsymbol{\psi}$ and f, also f will shortly be referred to as the characteristic map of the scheme. Using (15), we obtain for the segments of the characteristic map

$$f_j = \frac{1}{n} \sum_{\ell \in \mathbb{Z}_n} G_\ell(\cdot, j) w_n^{\ell k} \hat{v} = \frac{1}{n} \sum_{\ell \in \mathbb{Z}_n} G_{\ell-j}(\cdot, 0) w_n^{\ell k} \hat{v}$$

$$= \frac{w_n^{jk}}{n} \sum_{\ell \in \mathbb{Z}_n} G_\ell(\cdot, 0) w_n^{\ell k} \hat{v} = w_n^{jk} f_0.$$

This means that, due to shift invariance, all segments can be obtained from the first one by rotation. This observation leads immediately to a result concerning the appropriate Fourier index of the subdominant eigenvalue.

Theorem 6.3 *The characteristic map of a symmetric standard scheme can be injective only if $\mathcal{F}(\lambda) = \{1, n-1\}$.*

The proof is based on computing the winding number of curves in the image of f depending on k. Instead of going through the technical details, we refer to Figure 7,

22

which gives a good impression of the consequences of a wrong Fourier index. In the following, we will always assume that the complex eigenvector v according to (15) corresponds to the index $k = 1$. The index $n - 1$ leads to the complex conjugate eigenvector $\overline{v}$.

For a normalized characteristic map, flip invariance is exploited as follows: $AR = RA$ implies that also Rv is an eigenvector of A to λ, i.e., $Rv = av + b\overline{v}$ for some complex constants a, b. On one hand, by (14),

$$1 = G(2, 2, 0)v = G(2, 2, 0)Rv = a + b.$$

On the other hand, v and $\overline{v}$ are also eigenvectors of the shift matrix. With $Sv = w_n^{-1}v$ and $S\overline{v} = w_n\overline{v}$, we obtain

$$1 = G(2, 2, 0)v = G(2, 2, 0)SRSv = w_n^{-2}a + b.$$

The two conditions $a + b = w_n^{-2}a + b = 1$ have the unique solution $a = 0, b = 1$, i.e., $Rv = \overline{v}$. Hence,

$$f_0(s, t) = G(s, t, 0)v = G(t, s, 0)Rv = G(t, s, 0)\overline{v} = \overline{f_0(t, s)}.$$

We summarize our findings concerning symmetry properties of the characteristic map as follows:

Theorem 6.4 *Let $f = Gv$ be the normalized characteristic map of a symmetric standard scheme (A, G) derived via (15) from the eigenvector $\hat{v}$ of the block $\hat{A}_1$ to the subdominant eigenvalue λ. Then, for $j \in \mathbb{Z}_n$,*

$$f_j(s, t) = w_n^j f_0(s, t) = w_n^j \overline{f_0(t, s)} = \overline{f_{-j}(t, s)}. \tag{16}$$

The theorem tells us that the complete information on the characteristic map is essentially contained in one half of the first segment. More precisely, we define the *half domain*

$$\boldsymbol{\Sigma}_{\mathrm{h}} := \{(s, t) \in \boldsymbol{\Sigma} : s \leq t\},$$

and the *half segment* f_{h} as the restriction of the segment f_0 to this set. Obviously,

$${}^{\gamma}\!Df(s, t, j) = \begin{cases} {}^{\gamma}\!Df_{\mathrm{h}}(s, t) & \text{if } s \leq t \\ {}^{\gamma}\!Df_{\mathrm{h}}(t, s) & \text{if } s > t. \end{cases}$$

Thus, it suffices to verify ${}^{\gamma}\!Df_{\mathrm{h}} > 0$ to ensure regularity of the complete characteristic map. Since in a concrete setting ${}^{\gamma}\!Df_{\mathrm{h}}$ can be evaluated either numerically or even analytically, the required check of sign is typically easy to accomplish. By contrast, verifying injectivity seems to be a much harder task, and in most known proofs for specific algorithms, much effort is spent on that issue. The following theorem provides a significant simplification of the injectivity test.

Theorem 6.5 *Let (A, G) be a symmetric standard scheme with Fourier index $\mathcal{F} = \{1, n - 1\}$, and assume that the half segment f_{h} of the complex characteristic map f is normalized and regular. Then f is regular and injective if and only if all real points on the curve $\gamma_1(u) := f_{\mathrm{h}}(u, 1), u \in U$, are positive:*
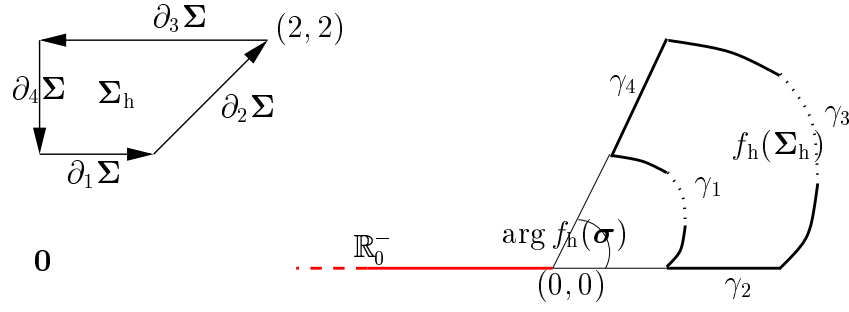
$$\gamma_1(U) \cap \mathbb{R}_0^- = \emptyset.$$

Figure 8: (*left*) Domain halfsegment $\boldsymbol{\Sigma}_{\mathrm{h}}$ and (*right*) spline image $f_{\mathrm{h}}(\boldsymbol{\Sigma}_{\mathrm{h}})$.

Proof   As already shown above, f is regular if and only if f_{h} is regular. If f is injective and $f_{\mathrm{h}}(u,1) \in \overline{\mathbb{R}_0^-}$, then, by Theorem 6.4, $f_{\mathrm{h}}(u,1) = f(1,u,0) = \overline{f(u,1,0)} = f(u,1,0)$. This implies $u = 1$, and with (12), the contradiction $0 > f(1,1,0) = \lambda f(2,2,0) = \lambda > 0$ follows. If all real points in $\gamma_1(U)$ are positive, we argue as follows:

First, we show that in this case also all real points in the image $f_{\mathrm{h}}(\boldsymbol{\Sigma}_{\mathrm{h}})$ are positive. To this end, we denote the four boundary segments of $\boldsymbol{\Sigma}_{\mathrm{h}}$ by $\partial_1\boldsymbol{\Sigma}, \ldots, \partial_4\boldsymbol{\Sigma}$, see Figure 8, *left*. The restrictions of f_{h} to these sets yield four boundary curves which we parametrize over $U = [0,1]$ by

$$\gamma_1(u) := f_{\mathrm{h}}(u,1), \qquad\qquad \gamma_2(u) := f_{\mathrm{h}}(1+u,1+u)$$
$$\gamma_3(u) := f_{\mathrm{h}}(2-2u,2), \qquad\qquad \gamma_4(u) := f_{\mathrm{h}}(0,2-u),$$

see Figure 8,*right*. By (12), the curves γ_1 and γ_3 are related according to $\gamma_1(u) = \lambda\gamma_3(1-u)$. By (16), $\gamma_2(u) = f_0(1+u,1+u) = \overline{f_0(1+u,1+u)}$ is real. Since f is regular, $\gamma_2' = Df_{\mathrm{h}}[1;1] \neq 0$. The endpoints are $\gamma_2(0) = \lambda$, $\gamma_2(1) = 1$. Hence, we conclude that $\gamma_2(u)$ is strictly monotone increasing and positive for all $u \in U$. Also by (16),

$$\gamma_4(u) = f_0(0,2-u) = \overline{f_0(2-u,0)} = \overline{f_{-1}(0,2-u)} = \overline{w_n^{-1} f_0(0,2-u)} = w_n \overline{\gamma_4(u)}.$$

This is possible only if $\gamma_4(u)$ lies on a straight line with angle either $\arg\gamma_4(u) = \pi/n$ or $\arg\gamma_4(u) = \pi + \pi/n$ for all $u \in U$. As before, one shows that $|\gamma_4(u)|$ is strictly monotone, and that $\gamma_4(u) \neq 0$ for all $u \in U$. Hence, $\gamma_4(U)$ does not contain real points. By assumption, $\gamma_1(U) \cap \overline{\mathbb{R}_0^-} = \emptyset$, and the same is true for $\gamma_3(U) = \gamma_1(U)/\lambda$. Together, we have shown that all real points on the image of the boundary of $\boldsymbol{\Sigma}_{\mathrm{h}}$ are positive, i.e., $f_{\mathrm{h}}(\partial\boldsymbol{\Sigma}_{\mathrm{h}}) \cap \overline{\mathbb{R}_0^-} = \emptyset$. Since, by the inverse function theorem, for a regular map the boundary of the image is a subset of the image of the boundary, we conclude that $f_{\mathrm{h}}(\boldsymbol{\Sigma}_{\mathrm{h}}) \cap \overline{\mathbb{R}_0^-} = \emptyset$

Second, we show that the minimum and maximum of the angle $\arg f_{\mathrm{h}}(\boldsymbol{\sigma})$ are attained if and only if $\boldsymbol{\sigma} \in \partial_2\boldsymbol{\Sigma}$ and $\partial_4\boldsymbol{\Sigma}$, respectively. Using the findings of the first part of the proof, we see that $\arg f_{\mathrm{h}} \in (-\pi,\pi)$ is well defined so that the search for extrema actually makes sense. Now, let $\boldsymbol{\sigma} \in \operatorname{argmin}\arg f_{\mathrm{h}}$ be an argument corresponding to the

24

minimal angle. As before, we conclude that $\boldsymbol{\sigma}$ has to lie on the boundary of $\boldsymbol{\Sigma}_{\mathrm{h}}$. If $\boldsymbol{\sigma}$ does not lie in $\partial_2\boldsymbol{\Sigma}\cup\partial_4\boldsymbol{\Sigma}$ then there exists $u \in (0,1)$ such that $\arg\gamma_1(u) = \arg\gamma_3(1-u)$ is minimal. Moreover, the tangents satisfy $\gamma_1'(u) = -\lambda\gamma_3'(1-u) \neq 0$. That is, the tangents point into opposite directions, while the image of f_{h} always lies on the left hand side of the boundary curve. Hence, there exists a point $\tilde{\boldsymbol{\sigma}}$ in the neighborhood either of $[u,1]$ or of $[2-2u,2]$ with $\arg f_{\mathrm{h}}(\tilde{\boldsymbol{\sigma}}) < \arg f_{\mathrm{h}}(\boldsymbol{\sigma})$ contradicting the minimality assumption. Analogously, one shows that $\operatorname{argmax}\arg f_{\mathrm{h}} \subset \partial_2\boldsymbol{\Sigma}\cup\partial_4\boldsymbol{\Sigma}$. Since the image of f_{h} lies on the left hand side of the curve γ_2, which is oriented from left to right on the positive real axis, we see that there exist positive angles so that $\arg\gamma_2 = 0$ cannot be maximal. Hence, $\min\arg f_{\mathrm{h}} = \arg\gamma_2 = 0$, and $\max\arg f_{\mathrm{h}} = \arg\gamma_4 = \pi/n$.

Third, we show that f_{h} is injective. Since the image $f_{\mathrm{h}}(\boldsymbol{\Sigma}_{\mathrm{h}})$ does not contain the origin, there exists $r \in \mathbb{N}$ such that $\lambda^r < |f_{\mathrm{h}}(\boldsymbol{\sigma})| \leq \lambda^{-r}$ for all $\boldsymbol{\sigma} \in \boldsymbol{\Sigma}_{\mathrm{h}}$. We define the domain $\boldsymbol{\Sigma}_{\mathrm{h}}^r := \cup_{|m|<r} 2^m\boldsymbol{\Sigma}_{\mathrm{h}}$ and the map

$$f_{\mathrm{h}}^r : \boldsymbol{\Sigma}_{\mathrm{h}}^r \ni \boldsymbol{\sigma} \mapsto \lambda^m f_{\mathrm{h}}(2^m\boldsymbol{\sigma}) \quad \text{if} \quad 2^m\boldsymbol{\sigma} \in \boldsymbol{\Sigma}_{\mathrm{h}}$$

consisting of scaled copies of f_{h}. This map is smooth and regular since consecutive parts satisfy contact conditions up to order k analogously to (13). The four boundary curves $\gamma_1^r, \ldots, \gamma_4^r$ of f_{h}^r are defined as shown in Figure 8,*right*. Now, we consider the function

$$\nu : \mathbb{C} \ni z \mapsto |\{\boldsymbol{\sigma} \in \boldsymbol{\Sigma}_{\mathrm{h}}^r : f_{\mathrm{h}}^r(\boldsymbol{\sigma}) = z\}| \in \mathbb{N}_0$$

assigning the number of pre-images to points in the complex plane. Since f_{h} is continuous, ν is upper semi-continuous. Since f_{h} is regular, ν is lower semi-continuous at all points not contained in the image $f_{\mathrm{h}}^r(\boldsymbol{\Sigma}_{\mathrm{h}}^r)$ of the boundary. From the results above it follows immediately that $\nu(\gamma_2(0)) = 1$. Further, by definition of r, the curves γ_1^r or γ_3^r do not intersect $f_{\mathrm{h}}(\boldsymbol{\Sigma}_{\mathrm{h}})$. Hence, ν is continuous and equal to one on $f_{\mathrm{h}}(\boldsymbol{\Sigma}_{\mathrm{h}})$.

Fourth, we show that f is injective. From

$$f(s,t,j) = \begin{cases} w_n^j f_{\mathrm{h}}(s,t) & \text{if } s \leq t \\ w_n^j f_{\mathrm{h}}(t,s) & \text{if } t \leq s \end{cases}$$

it follows

$$\arg f(s,t,j) \in \begin{cases} [0,\pi/n] + 2j\pi/n & \text{if } s \leq t \\ [-\pi/n, 0] + 2j\pi/n & \text{if } t \leq s. \end{cases}$$

For $(s,t,j) \neq (s',t',j')$, equal angles and moduli are only possible if $j' = j+1$ and $(s,t) = (t',s') \in \partial_4\boldsymbol{\Sigma}_{\mathrm{h}}$, or $j' = j$ and $(s,t) = (s',t') \in \partial_2\boldsymbol{\Sigma}_{\mathrm{h}}$, but these points are identified in $\mathbf{S}^0$. $\qquad\square$

Typically, the check for intersections of the curve γ_1 with the non-positive real line is easy to accomplish since, in case of injectivity, the angle of γ_1 varies between 0 and π/n, so that the two sets are not even close. We demonstrate the procedure in the next section at hand of the Doo-Sabin algorithm.
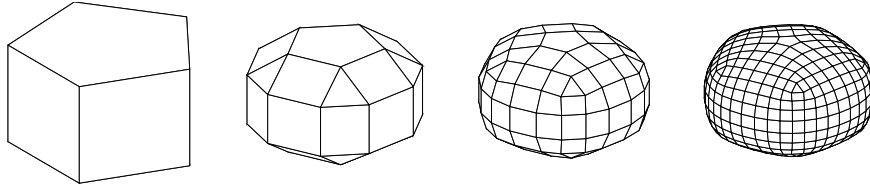
Figure 9: Mesh refinement of the Doo-Sabin algorithm.

Bibliographic Notes.

- The relevance of the Discrete Fourier Transform for the analysis of subdivision matrices was already recognized in [24].

- Symmetry properties of the characteristic map and their relation to its Fourier index are discussed in [63].

- In [99], an alternate criterion for injectivity of a regular characteristic map is given. It is based on the winding number of its boundary curve.

7 An example: The Doo-Sabin algorithm

The Doo-Sabin algorithm generalizes subdivision (uniform knot insertion) of biquadratic tensor-product B-splines. For each n-gon of the original mesh, a new, smaller n-gon is created and connected with its neighbors as depicted in Figure 9. Figure 10 shows the mask for generating a new n-gon from an old one for the regular case $n = 4$ (*left*) and the general case (*middle*). The standard weights suggested by Doo and Sabin in [24] are

$$a_j := \frac{\delta_{j,0}}{4} + \frac{3 + 2\cos(2\pi j/n)}{4n}. \tag{17}$$

Each of the n segments $\mathbf{x}_j^m$, $j \in \mathbb{Z}_n$, of the mth spline ring generated by the Doo-Sabin algorithm consists of three biquadratic B-spline patches. Accordingly, we can split the control points $\mathbf{Q}^m$ into n groups of nine control points, each, ordered as shown in Figure 10 (*right*). Since the scheme is symmetric, we can apply DFT as in Section 6 to obtain

$$\hat{A}_k = \begin{pmatrix} \hat{a}_k & 0 & 0 \\ \hat{A}_k^{1,0} & \hat{A}_k^{1,1} & 0 \\ \hat{A}_k^{2,0} & \hat{A}_k^{2,1} & 0 \end{pmatrix},$$

where $\hat{a}_k = \sum_j w_n^{-jk} a_j$ are the entries of the DFT of the vector $[a_0, \ldots, a_{n-1}]$ of inner weights. The sub-matrices $\hat{A}_k^{i,j}$ do not depend on the special choice of weights or on the index k. Rather, they contain information on the subdivision rules in the tensor
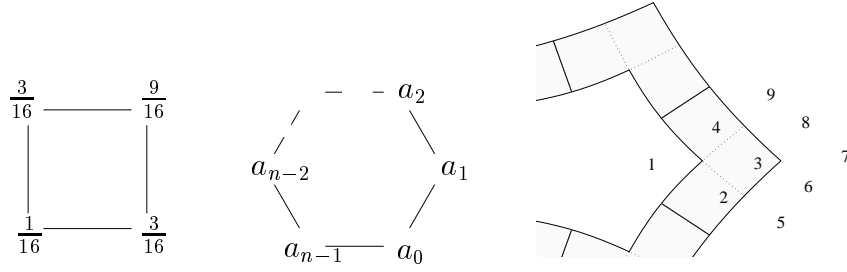
PSfrag replacements

Figure 10: Regular refinement rule (*left*), general refinement rule (*middle*), and labeling of the control points (*right*) of the Doo-Sabin algorithm.

product case. For instance,

$$\hat{A}_k^{1,1} = \frac{1}{16} \begin{bmatrix} 3 & 0 & \overline{w} \\ 3 & 1 & 3 \\ w & 0 & 3 \end{bmatrix}, \quad w := 16 w_n^k.$$

The weights a_j are assumed to sum to one, i.e., $\hat{a}_0 = 1$, and to be symmetric according to $a_j = a_{n-j}$, i.e., $\hat{a}_k = \hat{a}_{n-k}$ is real. The eigenvalues of $\hat{A}_k$ are $\hat{a}_k$, $1/4$, $1/8$, $1/16$, 0 so that the subdominant eigenvalue must be $\lambda := \hat{a}_1 = \hat{a}_{n-1} \in (1/4, 1)$. Using a computer algebra system, one can determine the complex eigenvector $\hat{v}$ of $\hat{A}_1$ corresponding to λ explicitly:

$$\hat{v} = \begin{bmatrix} 2\lambda(16\lambda-1)(8\lambda-1)(4\lambda-1) \\ 6\lambda(16\lambda-1)(6\lambda-1+2\overline{w_n}\lambda) \\ 18\lambda(32\lambda^2-1+4c_n\lambda) \\ 6\lambda(16\lambda-1)(6\lambda-1+2w_n\lambda) \\ (16\lambda-1)\left(12\lambda^2+18\lambda-3+\overline{w_n}(4\lambda^2+12\lambda-1)\right) \\ 6\lambda\left(32\lambda^2+64\lambda-12+c_n(20\lambda+1)-is_n(16\lambda-1)\right) \\ 64\lambda^3+512\lambda^2-46\lambda-8+36c_n\lambda(2\lambda+1) \\ 6\lambda\left(32\lambda^2+64\lambda-12+c_n(20\lambda+1)+is_n(16\lambda-1)\right) \\ (16\lambda-1)\left(12\lambda^2+18\lambda-3+w_n(4\lambda^2+12\lambda-1)\right) \end{bmatrix},$$

where $w_n = c_n + is_n$. In particular, for the original Doo-Sabin weights in (17), we have $\lambda = 1/2$ and, rearranging the entries of $\hat{v}$ in a (3×3)-matrix according to Figure 10, *right*,

$$\begin{bmatrix} \hat{v}_5 & \hat{v}_6 & \hat{v}_7 \\ \hat{v}_2 & \hat{v}_3 & \hat{v}_8 \\ \hat{v}_1 & \hat{v}_4 & \hat{v}_9 \end{bmatrix} = 3 \begin{bmatrix} 21+14\overline{w_n} & 28+2w_n+9\overline{w_n} & 35+12c_n \\ 14+\overline{7w_n} & 21+6c_n & 28+2\overline{w_n}+9w_n \\ 7 & 14+7w_n & 21+14w_n \end{bmatrix}.$$

By elementary computations, one can determine the Bernstein-Bézier-form of all three biquadratic patches forming the first segment of the complex characteristic map f. For $\lambda \in (1/4, 1)$, the minimum of the real parts of all Bernstein-Bézier coefficients is positive. Hence, by the convex hull property, the condition $\gamma_1(U) \cap \mathbb{R}_0^- = \emptyset$ is always satisfied. In particular, for $\lambda = 1/2$, we obtain the minimal value $\min \operatorname{Re} \gamma_1(U) =$

Re $f(0, 1, 0) = 21 + 21c_n > 0$. It remains to show regularity of the characteristic map. The Jacobian determinant $^{\lor}Df$ consists of three bicubic patches, which can also be expressed explicitly in Bernstein-Bézier-form. A careful analysis shows that all coefficients are positive if

$$p(\lambda) := 128\lambda^2(1 - \lambda) - 7\lambda - 2 + 9\lambda c_n > 0.$$

Again by the convex hull property, we conclude $^{\lor}Df > 0$ if $p(\lambda) > 0$. In particular, for $\lambda = 1/2$, we obtain $p(1/2) = 3/2\,(7 + 3c_n) > 0$ proving that the Doo-Sabin in its standard form is a C_1^1-scheme. Surprisingly, there is an upper bound $\lambda_{\sup}(n)$ with $p(\lambda) < 0$ for $1 > \lambda > \lambda_{\sup}(n)$. For such λ, $^{\lor}Df$ actually reveals a change of sign, and the corresponding algorithm cannot be C_1^1. Fortunately, the upper bounds are quite close to 1, so that they do not impose severe restrictions when designing variants on the standard Doo-Sabin algorithm. More precisely, the lowest upper bound occurs for $n = 3$,

$$\lambda_{\sup}(n) \geq \lambda_{\sup}(3) = \frac{\sqrt{187}}{24} \cos\left(\frac{1}{3} \arctan\left(\frac{27\sqrt{5563}}{1576}\right)\right) + \frac{1}{3} \approx 0.8773.$$

The asymptotic behavior for $n \to \infty$ is

$$\lambda_{\sup}(n) \doteq 1 - \frac{\pi^2}{7n^2}.$$

Summarizing, we have shown the following:

Theorem 7.1 *Let $\hat{a}_0, \ldots, \hat{a}_{n-1}$ be the Fourier coefficients of a symmetric set of weights for the generalized Doo-Sabin algorithm. Then a standard scheme is obtained if $\lambda := \hat{a}_1 = \hat{a}_{n-1}$ satisfies the condition*

$$1 > \lambda > \max\{1/4, |\hat{a}_2|, \ldots, |\hat{a}_{n-2}|\}.$$

The scheme is C_1^k if $p(\lambda) > 0$, and not C_1^k if $p(\lambda) < 0$. In particular, the scheme is C_1^k when choosing the standard weights.

Bibliographic Notes.

- Details of the analysis of the Doo-Sabin algorithms can be found in [63]. In the same paper, also the Catmull-Clark algorithm and possible generalizations are analyzed.

- Today, all relevant algorithms have been thoroughly analyzed. For instance, simplest subdivision in [62], Loop's scheme in [93], $\sqrt{3}$-subdivision in [45], and the butterfly scheme in [100].

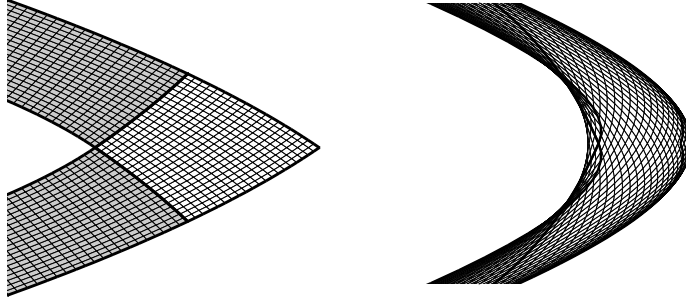- A quite universal algorithm for numerical verification has been provided in [99].

Figure 11: Characteristic map for $n = 3$ and subdominant eigenvalue (*left*) $\lambda = 0.5$ and (*right*) $\lambda = 0.95$.

8   Conditions for C_2^k-schemes

As we have shown, C_1^k-subdivision schemes are well understood and relatively easy to construct. By contrast, the development of schemes providing regularity of higher order is subject to very restrictive conditions on the eigenvalues and eigen-functions. In this section, we derive these conditions and discuss some of their consequences.

   While the central point $\mathbf{x}^c$ and the central normal $\mathbf{n}^c$ are determined by the eigen-coefficients $\mathbf{p}_0$ and $\mathbf{p}_1$, $\mathbf{p}_2$ related to the dominant and subdominant eigenvalue $\lambda_0 = 1$ and $\lambda_1 = \lambda_2 = \lambda$, curvature properties rely on the next smaller eigenvalue and the corresponding eigenfunctions. Let us assume that (A, G) is a standard C_2^2-scheme with eigenvalues

$$1 > \lambda > \mu := |\lambda_3| = \cdots = |\lambda_{\bar{q}}| > |\lambda_{\bar{q}+1}|$$

and, for the sake of simplicity, a full set of eigenvectors $v_3, \ldots, v_{\bar{q}}$ to the eigenvalues with modulus μ. The general case of non-trivial Jordan blocks is slightly more complicated from a purely technical point of view without providing further insight. Then the second order expansion of $\mathbf{x}^m$ reads

$$\mathbf{x}^m = GVJ^mV^{-1}\mathbf{Q} = FJ^m\mathbf{P} \doteq \mathbf{x}^c + \lambda^m \boldsymbol{\psi}[\mathbf{p}_1; \mathbf{p}_2] + \mu^m \mathbf{r}^m \tag{18}$$

with

$$\mathbf{r}^m := \sum_{q=3}^{\bar{q}} a_q^m f_q \mathbf{p}_q, \quad a_q := \lambda_q / \mu. \tag{19}$$

The sequences a_q^m have modulus 1 and account for the oscillating behavior of λ_q^m in the case when λ_q is negative or complex.

   For the rest of this section, the initial data are always assumed to be generic. Then, by definition of a C_2^2-scheme, the central height function h is twice differentiable at the origin. With H the symmetric (2×2)-matrix of second derivatives of h at the origin, also called the *central Hessian*, we obtain, using (4), the Taylor expansion

$$h(\boldsymbol{\xi}) = \frac{1}{2}\boldsymbol{\xi}H\boldsymbol{\xi}^{\mathrm{T}} + o(|\boldsymbol{\xi}|^2).$$

29

The mth spline ring of the projection $\boldsymbol{\xi}$ according to (2) is

$$\boldsymbol{\xi}^m(\mathbf{s}) = (\mathbf{x}^m(\mathbf{s}) - \mathbf{x}^c) \cdot \mathbf{T}^c \doteq \lambda^m \boldsymbol{\psi} L, \quad L := [\mathbf{p}_1; \mathbf{p}_2] \cdot \mathbf{T}^c, \tag{20}$$

where the (2×2)-matrix L has full rank. Since $[\mathbf{p}_1; \mathbf{p}_2] \cdot \mathbf{n}^c = \mathbf{0}$, the central height function according to (3) is $h(\boldsymbol{\xi}^m(\mathbf{s})) \doteq \mu^m \mathbf{r}^m(\mathbf{s}) \cdot \mathbf{n}^c$. Hence, after dividing (20) by λ^{2m}, we obtain the condition

$$\varrho^m \mathbf{r}^m \cdot \mathbf{n}^c = \boldsymbol{\psi} L H L^{\mathrm{T}} \boldsymbol{\psi}^{\mathrm{T}} + o(1 + \varrho^m), \quad \varrho := \mu/\lambda^2, \tag{21}$$

which has to be satisfied for an appropriate choice of H. By Lemma 4.1, the eigenfunctions f_q are non-zero implying that also $\mathbf{r}^m \cdot \mathbf{n}^c$ is in general non-zero. We distinguish three cases for the crucial ratio ϱ:

- If $\varrho < 1$, then $H = 0$ follows independent of the chosen data. This case of an enforced flat spot at the center will be referred to as *trivial curvature continuity*.

- If $\varrho = 1$, then the right hand side of (21) converges to a constant, and a simple argument shows that $\mathbf{r}^m \cdot \mathbf{n}^c$ can be constant only if $a_3 = \cdots = a_{\bar{q}} = 1$.

- If $\varrho > 1$, then the left hand side of (21) diverges faster than the right hand side, and asymptotic equality of the sequences is impossible.

Together, it follows that *non-trivial curvature continuity* is possible, although by no means guaranteed, only if

$$\lambda^2 = \mu = \lambda_3 = \cdots = \lambda_{\bar{q}}.$$

We call μ the *subsubdominant eigenvalue*, and elaborate on that case now. Passing to the limit, (21) reduces to

$$\sum_{q=3}^{\bar{q}} f_q p_q = \boldsymbol{\psi} L H L^{\mathrm{T}} \boldsymbol{\psi}^{\mathrm{T}}, \quad p_q := \mathbf{p}_q \cdot \mathbf{n}^c. \tag{22}$$

One can easily show that for any set of coefficients $p_3, \ldots, p_{\bar{q}}$ and arbitrary $\varepsilon > 0$ there exist generic initial data $\mathbf{Q}^\varepsilon$ such that the corresponding coefficients $p_3^\varepsilon, \ldots, p_{\bar{q}}^\varepsilon$ differ by less than ε. By continuity, we conclude that (22) holds for any choice of coefficients. In particular, for any $\ell = 3, \ldots, \bar{q}$, we can set $p_q := \delta_{q,\ell}$ to obtain

$$f_\ell = \boldsymbol{\psi} L H L^{\mathrm{T}} \boldsymbol{\psi}^{\mathrm{T}} = a f_1^2 + b f_2^2 + c f_1 f_2$$

for certain constants a, b, c. This means that all subsubdominant eigenfunctions must lie in the space of homogeneous quadratic polynomials in the two subdominant eigenfunctions. We summarize our findings as follows:

Theorem 8.1 *Let (A, G) be a standard C_2^2-scheme which is non-trivial in the sense that the central Hessian does not necessarily vanish. Then the subsubdominant eigenvalue μ satisfies*

$$\lambda^2 = \mu = \lambda_3 = \cdots = \lambda_{\bar{q}} > |\lambda_{\bar{q}+1}|,$$

and the subsubdominant eigenfunctions $f_3, \ldots, f_{\bar{q}}$ satisfy

$$f_\ell \in \mathrm{span}\{f_1^2, f_2^2, f_1 f_2\}. \tag{23}$$

It is not too difficult to construct subdivision schemes that have the desirable distribution of eigenvalues. By contrast, the conditions on the eigenfunctions are extremely restrictive and the major obstacle to remove when trying to construct C_2^k-schemes. Let us consider an implication on the important special case of piecewise polynomial subdivision surfaces. We define the bi-degree deg f of a spline ring $f \in C^k(\mathbf{S}^0, \mathbb{R}, G)$ as the maximal bi-degree of the polynomial pieces of f. For vector-valued spline rings, the bi-degree is the maximum over all components.

Theorem 8.2 *Let (A, G) be a standard C_2^k-scheme, and assume that the generating system consists of piecewise polynomials. If the scheme is flexible in the sense that there exist generic initial data such that the corresponding subdivision surface has positive Gaussian curvature at the center, then either $n = 4$ or*

$$\deg G \geq 2k + 2. \tag{24}$$

Proof First, we show deg $\boldsymbol{\psi} > k$ if $n \neq 4$. Suppose that deg $\boldsymbol{\psi} \leq k$. Then patches $\boldsymbol{\psi}_j$ of the characteristic map are not piecewise polynomial functions, but in fact single polynomials, which we now consider to be extended from $\boldsymbol{\Sigma}^0$ to all of $\mathbb{R}^2$. By means of the conditions (6), each patch $\boldsymbol{\psi}_{j+1}$ is completely determined by its predecessor $\boldsymbol{\psi}_j$, and we have
$$\boldsymbol{\psi}_{j+1}(s, t) = \boldsymbol{\psi}_j(-t, s), \quad j \in \mathbb{Z}_n.$$
Repeated use of this equation yields $\boldsymbol{\psi}_{j+4} = \boldsymbol{\psi}_j$. For the regular case $n = 4$ this is just fine, but otherwise it implies that the characteristic map is not injective contradicting Definition 5.5.

Positive Gaussian curvature means that $\det H > 0$. Hence, H is positive or negative definite. For generic initial data, L has full rank implying that LHL^{T} is positive or negative definite as well. We easily conclude for the degree of the scheme
$$\deg G = \deg(\boldsymbol{\psi} LHL^{\mathrm{T}} \boldsymbol{\psi}^{\mathrm{T}}) = 2 \deg \boldsymbol{\psi} \geq 2k + 2$$

since cancellation of the leading coefficients is impossible. $\qquad\square$

Since $k \geq 2$ for a scheme generating curvature continuous surfaces, we see that the simplest C_2^k-scheme has degree 6. Further, no scheme generalizing uniform B-spline subdivision, like the Catmull-Clark-scheme, comes into question because here $\deg G = k + 1 < 2k + 2$.

Bibliographic Notes.

- The case $\mu < \lambda^2$, which yields vanishing principal curvatures at the center, is discussed in [68]

- The importance of $\mu = \lambda^2$ for C_2^k has already been observed in [24].

- Necessity of (23) is proven in [74], and in [67], it could be shown that it is also sufficient. In the same paper, similar conditions for C_r^k-schemes are specified.

- In [74], it is pointed out that the degree estimate (24) relies on the piecewise polynomial structure of the surfaces rather than on properties of the subdivision algorithm. Thus, it applies even to non-stationary or non-linear schemes as long as they live up to certain symmetry properties.

- Generalizations of the degree estimate based on the concept of flexibility can be found in [69].

- C_2^k-algorithms, and even general C_r^k-algorithms are constructed in [66,76]. However, they are less elegant than the popular C_1^k-schemes and rarely used in practice.

9   Curvature analysis

In this section we discuss the limit behavior of curvature at the center. The results are useful to understand certain artifacts in subdivision surfaces, and provide insight for the construction of ameliorated schemes.

To conveniently analyze a subdivision surface $\mathbf{x}$ with eigencoefficients $\mathbf{P} = V^{-1}\mathbf{Q}$, we introduce a *local coordinate system* in $\mathbb{R}^3$ such that the center $\mathbf{x}^c =: \mathbf{0}$ is the origin, and the unit vectors are

$$\mathbf{e}_1 := \mathbf{p}_1/|\mathbf{p}_1|, \quad \mathbf{e}_2 := \mathbf{n}^c \times \mathbf{e}_1, \quad \mathbf{e}_3 := \mathbf{n}^c.$$

It is chosen such that the central tangent plane is spanned by $\mathbf{e}_1$ and $\mathbf{e}_2$. That is, the matrix $\mathbf{T}^c$ according to (2) is given by $\mathbf{T}^c := [\mathbf{e}_1; \mathbf{e}_2]$. As in Section 8, we assume

$$1 > \lambda > \mu := |\lambda_3| = \cdots = |\lambda_{\bar{q}}| > |\lambda_{\bar{q}+1}|$$

and a full set of eigenvectors $v_3, \ldots, v_{\bar{q}}$. The second order expansion of the spline rings according to (18) reads,

$$\mathbf{x}^m \doteq \lambda^m \boldsymbol{\psi}[\mathbf{p}_1; \mathbf{p}_2] + \mu^m \mathbf{r}^m$$

where $\mathbf{r}^m$ is defined by (19). With α the angle between $\mathbf{p}_1$ and $\mathbf{p}_2$, the first two components of $\mathbf{x}^m$ are asymptotically given by

$$\mathbf{x}^m \cdot \mathbf{T}^c \doteq \lambda^m \boldsymbol{\psi} L, \quad L := [\mathbf{p}_1; \mathbf{p}_2] \cdot \mathbf{T}^c = \begin{bmatrix} |\mathbf{p}_1| & 0 \\ |\mathbf{p}_2|\cos\alpha & |\mathbf{p}_2|\sin\alpha \end{bmatrix}, \tag{25}$$

while the third component is

$$\mathbf{x} \cdot \mathbf{n}^c \doteq \mu^m \mathbf{r}^m \cdot \mathbf{n}^c.$$

Assume that an eigenvalue λ_{q_0} with $|\lambda_{q_0}| = \mu$ is not positive. Then the sign of $\mathbf{r}^m \cdot \mathbf{n}^c$ is incessantly changing as $m \to \infty$ if $\mathbf{p}_{q_0} \cdot \mathbf{n}^c$ is large compared with the other coefficients $\mathbf{p}_q \cdot \mathbf{n}^c, q \in \{3, \ldots, \bar{q}\} \setminus \{q_0\}$. Schemes revealing such an oscillating behavior should be discarded, so that we focus now on the case of coinciding positive subsubdominant eigenvalues.

Definition 9.1 *A standard C_1^k-scheme with $k \geq 2$ and eigenvalues*

$$\lambda > \mu = \lambda_3 = \cdots = \lambda_{\bar{q}} > |\lambda_{\bar{q}+1}| \tag{26}$$

is called a (λ, μ)-scheme.

For a (λ, μ)-scheme, the real-valued spline rings $\mathbf{r}^m \cdot \mathbf{n}^c$ are independent of m, and we define

$$h^c := \mathbf{r}^m \cdot \mathbf{n}^c = \sum_{q=3}^{\bar{q}} f_q \mathbf{p}_q \cdot \mathbf{n}^c \in C^k(\mathbf{S}^0, \mathbb{R}). \tag{27}$$

Together, we find the expansion

$$\mathbf{x}^m \doteq [\lambda^m \boldsymbol{\psi} L, \mu^m h^c] = [\boldsymbol{\psi} L, h^c] \operatorname{diag}(\lambda^m, \lambda^m, \mu^m). \tag{28}$$

This means that, asymptotically, the spline rings $\mathbf{x}^m$ are just scaled copies of the surface $[\boldsymbol{\psi} L, h^c]$. For the forthcoming investigation of curvature and shape properties, this surface plays a most important role.

Definition 9.2 *The* central surface $\mathbf{z}^c$ *corresponding to the spline* $\mathbf{x} = B\mathbf{Q}$ *generated by a (λ, μ)-scheme is defined by*

$$\mathbf{z}^c := [\boldsymbol{\psi}^c, h^c] \in C^k(\mathbf{S}^0, \mathbb{R}^3), \quad \boldsymbol{\psi}^c := \boldsymbol{\psi} L,$$

where the (2×2)-matrix L and the real-valued spline ring h^c are given by (25) and (27), respectively.

It is important to notice that unlike the characteristic map, the central surface depends on the initial data. Using $\partial_1 := \partial_s, \partial_2 := \partial_t$, and the differential operators

$$D := \begin{bmatrix} \partial_1 \\ \partial_2 \end{bmatrix}, \quad D_{i,j} := \begin{bmatrix} D \\ \partial_i \partial_j \end{bmatrix},$$

the fundamental forms of a subdivision surface can be expressed conveniently.

Theorem 9.3 *For a (λ, μ)-scheme and generic initial data, the first fundamental form of the spline ring $\mathbf{x}^m$ and its inverse are given by*

$$I^m \doteq \lambda^{2m} I, \quad (I^m)^{-1} \doteq \lambda^{-2m} I^{-1}, \quad I := D\boldsymbol{\psi}^c \cdot D\boldsymbol{\psi}^c. \tag{29}$$

With I^c and II^c the first and second fundamental form of the central surface $\mathbf{z}^c$, the second fundamental form of $\mathbf{x}^m$ is

$$II^m \doteq \mu^m II, \quad II := \sqrt{\frac{\det I^c}{\det I}} \, II^c. \tag{30}$$

33

Proof The first formula follows immediately from $I^m = D\mathbf{x}^m \cdot D\mathbf{x}^m$, $D\mathbf{x}^m \doteq \lambda^m D\boldsymbol{\psi}^c \mathbf{T}^c$, and $\mathbf{T}^c \cdot \mathbf{T}^c = \mathrm{Id}$. To compute the inverse, we note that

$$\det I = (^{\times}\!D\boldsymbol{\psi}^c)^2 = (^{\times}\!D\boldsymbol{\psi})^2 (\det L)^2 = (^{\times}\!D\boldsymbol{\psi})^2 \, |\mathbf{p}_1 \times \mathbf{p}_2|^2.$$

For generic initial data, the cross product does not vanish, while $(^{\times}\!D\boldsymbol{\psi})^2 \geq c > 0$ for some constant c by regularity of $\boldsymbol{\psi}$, compactness of the domain, and continuity of $^{\times}\!D\boldsymbol{\psi}$. Hence,

$$(\det I^m)^{-1} \doteq \lambda^{-4m} (\det I)^{-1}$$

and the formula for $(I^m)^{-1}$ follows easily.

From (28), we conclude

$$\det D_{i,j}\mathbf{x}^m \doteq \lambda^{2m} \mu^m \det D_{i,j}\mathbf{z}^c,$$

and (30) is obtained by comparing the definitions

$$II_{i,j}^m = \frac{\det D_{i,j}\mathbf{x}^m}{\sqrt{\det I^m}}, \quad II_{i,j}^c = \frac{\det D_{i,j}\mathbf{z}^c}{\sqrt{\det I^c}}.$$

$\square$

It is important to notice that the second fundamental form of $\mathbf{x}^m$ and the central surface $\mathbf{z}^c$ differ only be a scalar factor. For that reason, their shape properties are closely related. With the help of the fundamental forms we can compute the *Weingarten map*, which in turn determines the asymptotic behavior of the principal curvatures and directions. We recall that the Weingarten map (also known as the *shape operator*) is defined as the differential of the normal map. Its eigenvalues are the principal curvatures, while its left eigenvectors in the parameter domain are mapped to the principal directions by the Jacobian of the surface parametrization.

Theorem 9.4 *For a (λ, μ)-scheme and generic initial data, the Weingarten map W^m of $\mathbf{x}^m$ is*

$$W^m \doteq \varrho^m W, \quad W := II\, I^{-1}, \quad \varrho := \frac{\mu}{\lambda^2}. \tag{31}$$

Let Q be the matrix of normalized left eigenvectors and K the diagonal matrix of eigenvalues of W,

$$W = Q^{-1}KQ. \tag{32}$$

The diagonal matrix of principal curvatures $K^m := \mathrm{diag}(\kappa_1^m, \kappa_2^m)$ of $\mathbf{x}^m$ is given by

$$K^m \doteq \varrho^m K, \tag{33}$$

while the principal directions $\mathbf{P}^m := [\mathbf{p}_1^m; \mathbf{p}_2^m]$ converge to the $\mathbf{e}_1\mathbf{e}_2$-plane:

$$\mathbf{P}^m \doteq \mathbf{P}, \quad \mathbf{P} := Q\, D\boldsymbol{\psi}^c\, \mathbf{T}^c. \tag{34}$$

Proof With respect to the parameter domain, the Weingarten map is given by $W^m := II^m (I^m)^{-1}$, and (31) follows from (29) and (30). The principal curvatures κ_1^m, κ_2^m are the eigenvalues of W^m, and that implies (33). The matrix Q^m of normalized left eigenvectors of W^m converges according to $Q^m \doteq Q$. Further, by (28), $D\mathbf{x}^m \doteq \lambda^m D\boldsymbol{\psi}^c \mathbf{T}^c$. Hence, using appropriate scaling, the principal directions of $\mathbf{x}^m$ are $\mathbf{P}^m = \lambda^{-m} Q D\mathbf{x}_m \doteq Q \, D\boldsymbol{\psi} \, \mathbf{T}^c$, as stated. $\qquad\square$

As in the preceding section, we see that the ratio ϱ plays a central role for the limit behavior of curvature.

Theorem 9.5 *For a (λ, μ)-scheme and generic initial data, the principal curvatures near the center behave according to the ratio ϱ.*

- *If $\varrho < 1$, then both principal curvatures converge to 0.*

- *If $\varrho = 1$, then both principal curvatures are bounded and at least one of them does not converge to 0.*

- *If $\varrho > 1$, then at least one principal curvature diverges.*

Proof In view of (33), it remains to show that $K \neq 0$ for generic initial data. If $K = 0$, then $W = 0$ and $II = II^c = 0$. The second fundamental form II^c of $\mathbf{z}^c$ vanishes only if $\mathbf{z}^c$ is planar. This is the case if and only if h^c and $\boldsymbol{\psi}$ are linearly dependent, i.e., if there are constants $a, b, c \in \mathbb{R}$ which do not vanish simultaneously, such that

$$ah^c + \boldsymbol{\psi}[b; c] = 0.$$

Let $\mathbf{s} = (s, t, j)$ be an arbitrary point on the outer boundary of the domain $\mathbf{S}^0$, i.e., $\max\{s, t\} = 2$. Then, by (12), $\boldsymbol{\psi}(2^{-1}\mathbf{s}) = \lambda\boldsymbol{\psi}(\mathbf{s})$. Analogously, since h^c is an eigenfunction to μ, one can show $h^c(2^{-1}\mathbf{s}) = \mu h^c(\mathbf{s})$. Hence,

$$ah^c(\mathbf{s}) + \boldsymbol{\psi}(\mathbf{s})[b; c] = 0$$
$$a\mu h^c(\mathbf{s}) + \lambda\boldsymbol{\psi}(\mathbf{s})[b; c] = 0.$$

This implies $\boldsymbol{\psi}(\mathbf{s})[b; c] = 0$. Let us assume that $[b; c] = [0; 0]$. Then $a \neq 0$ and $h^c = 0$. By Lemma 4.1, the eigenfunctions $f_3, \ldots, f_{\bar{q}}$ to μ are linearly independent so that all coefficients $\mathbf{p}_q \cdot \mathbf{n}^c$ in the definition (27) of h^c must vanish. This contradicts the assumption that the initial data are generic. Now, we assume $[b; c] \neq [0; 0]$. In this case, all outer boundary points $\boldsymbol{\psi}(\mathbf{s})$ lie on the straight line $xb + yc = 0$. Since $\boldsymbol{\psi}(2^{-1}\mathbf{s}) = \lambda\boldsymbol{\psi}(\mathbf{s})$, also all inner boundary points lie on the same straight line. Since $\boldsymbol{\psi}$ is regular, the boundary of the image is a subset of the image of the boundary, which is part of a straight line. Hence, the complete image of $\boldsymbol{\psi}$ must be part of a straight line; but this is impossible for a regular map. $\qquad\square$

In the last section, we have derived a necessary condition for C_2^k-schemes. Now, we are able to show that this condition is also sufficient.

Theorem 9.6 *A (λ, μ)-scheme is C_2^k if and only if $\mu = \lambda^2$ and the subsubdominant eigenfunctions $f_3, \ldots, f_{\bar{q}}$ satisfy*

$$f_\ell \in \mathrm{span}\{f_1^2, f_2^2, f_1 f_2\}.$$

Proof   In Theorem 8.1, we have shown that the given conditions are necessary. Now, let us assume that they are satisfied. Then there exists a symmetric (2×2)-matrix S with constant entries such that

$$h^{\mathrm{c}} = \frac{1}{2}\, \boldsymbol{\psi}^{\mathrm{c}} S \cdot \boldsymbol{\psi}^{\mathrm{c}}.$$

It is easily verified by inspection that

$$I = D\boldsymbol{\psi}^{\mathrm{c}} \cdot D\boldsymbol{\psi}^{\mathrm{c}}, \quad II = D\boldsymbol{\psi}^{\mathrm{c}} S \cdot D\boldsymbol{\psi}^{\mathrm{c}}.$$

Hence, by (31), $W = II\, I^{-1} = D\boldsymbol{\psi}^{\mathrm{c}}\, S\, (D\boldsymbol{\psi}^{\mathrm{c}})^{-1}$. That is, the eigenvalues of S and W coincide and are constant. More precisely, if $S = RKR^{-1}$ for a diagonal matrix K, then

$$W = Q^{-1}KQ, \quad Q := (D\boldsymbol{\psi}\, R)^{-1}.$$

Comparison with (32) shows that the principal curvatures converge according to $K^m \doteq K$. By (34), also the principal directions converge to a constant limit:

$$\mathbf{P}^m \doteq Q\, D\boldsymbol{\psi}\, \mathbf{T}^{\mathrm{c}} = R^{-1}\, \mathbf{T}^{\mathrm{c}}.$$

$\square$

We conclude our discussion of the limit behavior of curvature by specifying limit exponents for L^p-integrability. More precisely, for $1 \le p \le \infty$, we say that a subdivision surface is $H_{2,p}^k$, if it is C_1^k, and if the principal curvatures are L^p-integrable when restricted to a sufficiently small neighborhood of the center.

Theorem 9.7 *For a (λ, μ)-scheme and generic initial data, the generated subdivision surface is*

- $H_{2,\infty}^k$, *if $\varrho \le 1$.*
- $H_{2,p}^k$ *for all $p < -2\log \lambda / \log \varrho$, if $\varrho > 1$.*

In particular, for any ϱ, the surface is $H_{2,2}^k$.

Proof For $\varrho \le 1$, the principal curvatures are bounded, as stated. For $\varrho > 1$, we choose m_0 so large that I^m is regular for all $m \ge m_0$. Then, with the surface element $d\mathbf{x}^m = \sqrt{\det I^m}\, ds\, dt \doteq \lambda^{2m} \sqrt{\det I}\, ds\, dt$, the surface integral of the pth power of the principal curvatures of the mth spline ring is

$$\int_{\mathbf{x}^m} |K^m|^p d\mathbf{x}^m \doteq \varrho^{mp} \lambda^{2m} \bar{K}, \quad \bar{K} := \sum_{j \in \mathbb{Z}_n} \int_{\mathbf{\Sigma}^0} K_j \sqrt{\det I_j}\, ds\, dt,$$

where K_j and I_j denote the jth segment of K and I, respectively. Summing over all $m \ge m_0$, we obtain

$$\sum_{m=m_0}^{\infty} \int_{\mathbf{x}^m} |K^m|^p d\mathbf{x}^m \doteq \frac{(\varrho^p \lambda^2)^{m_0} \bar{K}}{1 - \varrho^p \lambda^2},$$

which is finite for $p < -2 \log \lambda / \log \varrho$. Since $\varrho < \lambda^{-1}$, the upper bound is always ≥ 2. $\qquad\qquad \square$

Bibliographic Notes.

- A first careful analysis of curvature in a vicinity of the center was given in [59], and bounds on their oscillation were specified in [60].

- The concept of the central surface and its relation to the limit behavior of curvature was introduced in [64]. Applications of the theory are discussed in [40].

- The basic limit behavior of principal curvatures according to Theorem 9.5 was observed in [24, 52, 64].

- L^p-regularity of principal curvatures was investigated in [79]. The results of Theorem 9.7 are crucial for using subdivision surfaces in the finite element analysis of higher order problems as in [12, 13].

- The central surface provides further information on the local shape of a subdivision surface near the center. The analysis in [64] shows that the subsubdominant eigenvalue μ must be at least triple with Fourier index $\{0, 2, n-2\} \subset \mathcal{F}(\mu)$ in order to avoid severe restrictions on what type of shapes can be modeled.

- If $\mathcal{F}(\mu) = \{0, 2, n-2\}$, [40] defines a chart that characterizes, for a subdivision algorithm and for the full gamut of input data, the shape of resulting surfaces.

10 Conclusion

Subdivision surfaces are remarkably similar to spline surfaces. Their distinct character reveals itself in the neighborhood of extraordinary points where $n \ne 4$ quadrilateral

patches join. This paper summarizes the structure of subdivision surfaces near extraordinary points. It adds two new building blocks to the foundations by clarifying the role of linearly dependent generating systems and simplifying the test for injectivity of the characteristic map.

References

[1] M. Alexa. Refinement operators for triangle meshes. *Computer Aided Geometric Design*, 19(4):169–172, 2002.

[2] C. Bajaj, S. Schaefer, J. Warren, and G. Xu. A subdivision scheme for hexahedral meshes. *The Visual Computer*, 18(5-6):343–356, 2002.

[3] A.A. Ball and D.J.T. Storry. A matrix approach to the analysis of recursively generated B-spline surfaces. *Computer Aided Design*, 18:437–442, 1986.

[4] A.A. Ball and D.J.T. Storry. Conditions for tangent plane continuity over recursively generated b-spline surfaces. *ACM Trans. on Graphics*, 7:83–102, 1988.

[5] A.A. Ball and D.J.T. Storry. An investigation of curvature variations over recursively generated B-spline surfaces. Technical report, Loughborough University of Technology, 1990.

[6] L. Barthe, C. Gérot, M. Sabin, and L. Kobbelt. Simple computation of the eigencomponents of a subdivision matrix in the fourier domain. In *Advances in Multiresolution for Geometric Modelling, N.A. Dodgson, M.S. Floater, and M.A. Sabin (eds), Springer*, 245–258, 2005.

[7] H. Biermann, A. Levin, and D. Zorin. Piecewise smooth subdivision surfaces with normal control. In *SIGGRAPH 2000 Conference Proceedings: Computer Graphics Annual Conference Series*, 113–120, 2000.

[8] W. Böhm. Subdividing multivariate splines. *Computer Aided Design*, 15(6):345–352, 1983.

[9] E. Catmull and J. Clark. Recursively generated B-spline surfaces on arbitrary topological meshes. *Computer Aided Design*, 10:350–355, 1978.

[10] A.S. Cavaretta, W. Dahmen, and C.A. Micchelli. Stationary subdivision. *Memoirs of the American Mathematical Society*, 93(453):1–186, 1991.

[11] G.M. Chaikin. An algorithm for high-speed curve generation. *Computer Graphics and Image Processing*, 3:346 − 349, 1974.

[12] F. Cirak, M.J. Scott, E.K. Antonsson, M. Ortiz, and P. Schröder. Integrated modeling, finite element analysis and engineering design for thin-shell structures using subdivision. *Computer Aided Design*, 34:137–148, 2002.

[13] F. Cirak, M. Ortiz, and P. Schröder. Subdivision surfaces: A new paradigm for thin-shell finite element analysis. *Int. J. Numer. Meth. Eng.*, 47(12):2039–2072, 2000.

[14] D. Cohen-Steiner, P. Alliez, and M. Desbrun. Variational shape approximation. *ACM Trans. Graph.*, 23(3):905–914, 2004.

[15] C. Conti and G. Zimmermann. Interpolaroy rank-1 vector subdivision schemes. *Computer Aided Geometric Design*, 21:341–351, 2004.

[16] W. Dahmen, N. Dyn, and D. Levin. On the convergence rates of subdivision algorithms for box splines. *Constructive Approximation*, 1:305–322, 1985.

[17] W. Dahmen and C.A. Micchelli. Subdivision algorithms for the generation of box splines. *Comp. Aided Geom. Design*, 1:77–85, 1984.

[18] R. van Damme. Bivariate hermite subdivision. *Computer Aided Geometric Design*, 14:847–875, 1997.

[19] T. DeRose, M. Halstead, and M. Kass. Efficient, fair interpolation using Catmull-Clark surfaces. In *SIGGRAPH '93 Proc.*, 35–44. Apple Computer, Inc., 1993.

[20] T. DeRose, M. Kass, and T. Truong. Subdivision surfaces in character animation. In *SIGGRAPH 1998 Conference Proceedings: Computer Graphics Annual Conference Series*, 85–94, 1998.

[21] N. Dodgson, I. Ivrissimtzis, and M. Sabin. Characteristics of dual triangular $\sqrt{3}$ subdivision. In *Curve and Surface fitting: St Malo 2002*, 119–128, 2003.

[22] N. Dodgson, M. Sabin, L. Barthe, and M. Hassan. Towards a ternary interpolating scheme for the triangular mesh. Technical Report UCAM-CL-TR-539, Computer Laboratory, University of Cambridge, 2002.

[23] D. Doo. A subdivision algorithm for smoothing down irregularly shaped polyhedrons. In *Proc. Int'l Conf. on Interactive Techniques in Computer Aided Design, IEEE Computer Soc.*, 157–165, 1978.

[24] D. Doo and M.A. Sabin. Behaviour of recursive subdivision surfaces near extraordinary points. *Computer Aided Design*, 10:356–360, 1978.

[25] S. Dubuc. Interpolation through an iterative scheme. *J. Math. Anal. Appl.*, 114:185–204, 1986.

[26] N. Dyn. Using laurent polynomial representation for the analysis of non-uniform binary subdivision schemes. *Adv. Comput. Math.*, 11:41–54, 1999.

[27] N. Dyn, J.A. Gregory, and D. Levin. A four-point interpolatory subdivision scheme for curve design. *Comp. Aided Geom. Design*, 4:257–268, 1987.

[28] N. Dyn, J.A. Gregory, and D. Levin. Analysis of uniform binary subdivision schemes for curve design. *Constructive Approximation*, 7:127–147, 1991.

[29] N. Dyn and D. Levin. Analysis of asymptotically equivalent binary subdivision schemes. *Journal of Math.Anal.Appl.*, 193:594–621, 1995.

[30] N. Dyn and D. Levin. Subdivision schemes in geometric modelling. *Acta Numerica*, 73–144, 2002.

[31] N. Dyn, D. Levin, and J.A. Gregory. A butterfly subdivision scheme for surface interpolation with tension control. *ACM Transactions on Graphics*, 9:160–169, 1990.

[32] N. Dyn, D. Levin, and D. Liu. Interpolatory convexity-preserving subdivision schemes for curves and surfaces. *Computer Aided Design*, 24:211–216, 1992.

[33] C. Gérot, L. Barthe, N. Dodgson, and M. Sabin. Subdivision as a sequence of sampled C^p surfaces. In *Advances in Multiresolution for Geometric Modelling, N.A. Dodgson, M.S. Floater, and M.A. Sabin (eds), Springer*, 259–270, 2005.

[34] B. Han. Computing the smoothness exponent of a symmetric multivariate refinable function. *SIAM Journal on Matrix Analysis and its Applications*, 24:693–714, 2003.

[35] M. Hassan, I.P. Ivrissimtzis, N. Dodgson, and M. Sabin. An interpolating 4-point c^2 ternary stationary subdivision scheme. *Computer Aided Geometric Design*, 19:1–18, 2002.

[36] F. Holt. Towards a curvature-continuous stationary subdivision algorithm. *Z. Angew. Math. Mech.*, 76, 1995.

[37] I.P. Ivrissimtzis, N. Dodgson, and M. Sabin. $\sqrt{5}$ subdivision. In *Advances in Multiresolution for Geometric Modelling, N.A. Dodgson, M.S. Floater, and M.A. Sabin (eds), Springer*, 285–299, 2005.

[38] I.P. Ivrissimtzis, K. Shrivastava, and H-P. Seidel. Subdivision rules for general meshes. In *St Malo 2002*, 229–237, 2003.

[39] I.P. Ivrissimtzis, M. Sabin, and N. Dodgson. On the support of recursive subdivision surfaces. Technical Report UCAM-CL-TR-544, Computer Laboratory, University of Cambridge, 2002.

[40] K. Karciauskas, J. Peters, and U. Reif. Shape characterization of subdivision surfaces – case studies. *Computer Aided Geometric Design*, 21(6):601–614, 2004.

[41] L. Kobbelt. Interpolatory refinement by variational methods. In C. Chui and L. Schumaker, editors, *Approximation Theory VIII, Vol. 2: Wavelets and Multilevel Approximation*, 217–224. World Scientific Publishing Co., 1995.

[42] L. Kobbelt. Interpolatory subdivision on open quadrilateral nets with arbitrary topology. *Computer Graphics Forum*, 15:409–420, 1996.

[43] L. Kobbelt. A variational approach to subdivision. *Comp. Aided Geom. Design*, 13:743–761, 1996.

[44] L. Kobbelt. Using the discrete Fourier-transform to analyze the convergence of subdivision schemes. *Appl. Comp. Harmonic Anal.*, 5:68–91, 1998.

[45] L. Kobbelt. $\sqrt{3}$ subdivision. In *Proceedings of ACM SIGGRAPH 2000*, 103–112, 2000.

[46] J.M. Lane and R.F. Riesenfeld. A theoretical development for the computer generation of piecewise polynomial surfaces. *IEEE Trans. Pattern Anal. Machine Intell.*, 2:35–46, 1980.

[47] M. Leber. Interpolierende Unterteilungsalgorithmen. Master's thesis, Universität Stuttgart, 1994.

[48] A. Levin. *Combined subdivision schemes.* PhD thesis, Tel-Aviv University, 1999.

[49] A. Levin. Combined subdivision schemes for the design of surfaces satsifying boundary conditions. *CAGD*, 16:345–354, 1999.

[50] N. Litke, A. Levin, and P. Schröder. Trimming for subdivision surfaces. *CAGD*, 18:463–481, 2001.

[51] C. Loop. Bounded curvature triangle mesh subdivision with the convex hull property. *The Visual Computer*, 18(5-6):316–325, 2002.

[52] Ch.T. Loop. Smooth subdivision for surfaces based on triangles. Master's thesis, University of Utah, 1987.

[53] C.A. Micchelli and H. Prautzsch. Computing curves invariant under halving. *Comp. Aided Geom. Design*, 4:133–140, 1987.

[54] C.A. Micchelli and H. Prautzsch. Computing surfaces invariant under subdivision. *Comp. Aided Geom. Design*, 4:321–328, 1987.

[55] G. Morin, J. Warren, and H. Weimer. A subdivision scheme for surfaces of revolution. *CAGD*, 18(5):483–502, 2001.

[56] A. Nasri and M. Sabin. Taxonomy of interpolation constraints on recursive subdivision curves. *The Visual Computer*, 18:259–272, 2002.

[57] P. Oswald and P. Schröder. Composite primal/dual $\sqrt{3}$ subdivision schemes. *CAGD*, 20:135–164, 2003.

[58] J. Peters. Geometric continuity. In *Handbook of Computer Aided Geometric Design*, 193–229. Elsevier, 2002.

[59] J. Peters and G. Umlauf. Gaussian and mean curvature of subdivision surfaces. In *The Mathematics of Surfaces IX, Cipolla and Martin (eds), Springer 2000, ISBN 1-85233-358-8*, 59–69, 2000.

[60] J. Peters and G. Umlauf. Computing curvature bounds for bounded curvature subdivision. *CAGD*, 18:455–461, 2001.

[61] J. Peters and L-J. Shiue. 4-3 directionally ripple-free subdivision. *ACM Transactions on Graphics*, 2003.

[62] J. Peters and U. Reif. The simplest subdivision scheme for smoothing polyhedra. *ACM Transactions on Graphics*, 16:420–431, 1997.

[63] J. Peters and U. Reif. Analysis of algorithms generalizing B-spline subdivision. *SIAM Journal on Numerical Analysis*, 35(2):728–748, 1998.

[64] J. Peters and U. Reif. Shape characterization of subdivision surfaces: basic principles. *Comput. Aided Geom. Des.*, 21(6):585–599, 2004.

[65] J. Peters and X. Wu. On the local linear independence of generalized subdivision functions. *submitted*.

[66] H. Prautzsch. Freeform splines. *Comp. Aided Geom. Design*, 14:201–206, 1997.

[67] H. Prautzsch. Smoothness of subdivision surfaces at extraordinary points. *Adv. in: Comp. Math.*, 9:377–390, 1998.

[68] H. Prautzsch and G. Umlauf. Improved triangular subdivision schemes. In *Proc Computer Graphics International*, 626–632, 1998.

[69] H. Prautzsch and U. Reif. Necessary conditions for subdivision surfaces. *Advances in Computational Mathematics*, 10:209–217, 1999.

[70] K. Qin and H. Wang. Eigenanalysis and continuity of non-uniform Doo-Sabin surfaces. In *Proc Pacific Graphics 99*, 179–186, 1999.

[71] U. Reif. *Neue Aspekte in der Theorie der Freiformflächen beliebiger Topologie*. PhD thesis, Universität Stuttgart, 1993.

[72] U. Reif. Some new results on subdivision algorithms for meshes of arbitrary topology. In C. K. Chui and L. L. Schumaker, editors, *Wavelets and Multilevel Approximation*, volume 2 of *Series in Approximations and Decompositions*, 367–374. World Scientific, 1995.

[73] U. Reif. A unified approach to subdivision algorithms near extraordinary vertices. *Comp. Aided Geom. Design*, 12:153–174, 1995.

[74] U. Reif. A degree estimate for subdivision surfaces of higher regularity. *Proc. of the AMS*, 124(7):2167–2174, 1996.

[75] U. Reif. A refineable space of smooth spline surfaces of arbitrary topological genus. *Journal of Approximation Theory*, 90(2):174–199, 1997.

[76] U. Reif. TURBS – Topologically unrestricted rational B-splines. *Constructive Approximation*, 14:57–77, 1998.

[77] U. Reif. *Analyse und Konstruktion von Subdivisionsalgorithmen für Freiform-flächen beliebiger Topologie*. Shaker Verlag, 1999. Habilitationsschrift.

[78] U. Reif and J. Peters. Structural analysis of subdivision surfaces. in preparation.

[79] U. Reif and P. Schröder. Curvature smoothness of subdivision surfaces. *Advances in Computational Mathematics*, 14(2):157–174, 2001.

[80] M. Sabin. Recursive division. In J. Gregory, editor, *The Mathematics of Surfaces*, 269–282. Clarendon Press, Oxford, 1986.

[81] M. Sabin. Cubic recursive division with bounded curvature. In *Curves and Surfaces ed Schumaker, Laurent and LeMehaute (eds) Academic Press.*, 411–414, 1991.

[82] M. Sabin. Eigenanalysis and artifacts of subdivision curves and surfaces. In *Primus Workshop Proceedings*, 69–92, 2002.

[83] M. Sabin. Subdivision surfaces. *in Handbook of Computer Aided Design*, 309–326, 2002.

[84] M. Sabin, N. Dodgson, M. Hassan, and I. Ivrissimtzis. Curvature behaviours at extraordinary points of subdivision surfaces. *CAD*, 1047–1051, 2003.

[85] M. Sabin and L. Barthe. Artifacts in recursive subdivision surfaces. In *St Malo 2002*, 353–362, 2003.

[86] S. Schaefer and J. Warren. On C^2 triangle/quad subdivision. *ACM TOG*, to appear.

[87] P. Schröder. Subdivision as a fundamental bulding block of digital geometry processing algorithms. *J Comput. Appl.Math.*, 149(1):207–219, 2002.

[88] L. Shiue and J. Peters. Mesh Refinement based on Euler Encoding, in *Proceedings of The International Conference on Shape Modeling and Applications*, 1–6, 2005.

[89] L. Shiue and I. Jones and J. Peters. A Realtime GPU Subdivision Kernel, *ACM Siggraph 2005, Computer Graphics Proceedings*, M. Gross editor, 1–6, 2005.

[90] J. Stam. Exact evaluation of catmull-clark subdivision surfaces at arbitrary parameter values. In *Proceedings of SIGGRAPH 1998*, 395–404, 1998.

[91] J. Stam. On subdivision schemes generalizing uniform b-spline surfaces of arbitrary degree. *CAGD*, 18:383–396, 2001.

[92] D.J.T. Storry. *B-spline surfaces over an irregular topology by recursive subdivision*. PhD thesis, 1985.

[93] G. Umlauf. Analyzing the characteristic map of triangular subdivision schemes. *CA*, 16(1):145–155, 2000.

[94] L. Velho. Quasi 4-8 subdivision. *Computer Aided Geometric Design*, 18(4):345–358, 2001.

[95] L. Velho and D. Zorin. 4-8 subdivision. *Computer Aided Geometric Design*, 18(5):397–427, 2001.

[96] J. Warren and H. Weimer. *Subdivision Methods for Geometric design*. Morgan Kaufmann, 2002.

[97] J. Warren and S. Schäfer. A factored approach to subdivision surfaces. *Computer graphics and applications, IEEE*, 24:74–81, 2004.

[98] D. Zorin. *Subdivision and multiresolution surface representations*. PhD thesis, Caltech, Pasadena, 1997.

[99] D. Zorin. Smoothness of stationary subdivision on irregular meshes. *Constr. Approx.*, 16(3):359–397, 2000.

[100] D. Zorin, P. Schröder, and W. Sweldens. Interpolatory subdivision for meshes with arbitrary topology. In *Proc ACM SIGGRAPH 1996*, 189–192, 1996.

[101] D. Zorin and P. Schröder. A unified framework for primal/dual quadrilateral subdivision schemes. *CAGD*, 18:429–454, 2001.